Synthesis and Structural and Electronic Properties of the Mixed Complexes of Vinylene-Bridged Bis- and Tris(octaethylporphyrin)s with Ni(II), Pd(II), and Pt(II) Ions

Hiroyuki Higuchi,* Masatoshi Shinbo, Masanobu Usuki, Makoto Takeuchi, Keita Tani,† and Koji Yamamoto

Department of Chemistry, Faculty of Science, Toyama University, 3190 Gofuku, Toyama, Toyama 930-8555

†Division of Natural Science, Osaka Kyoiku University, 4-698-1 Asahi-oka, Kashiwara, Osaka 582-0026

(Received December 27, 1999)

Various mixed complexes of vinylene-bridged bis- and tris(octaethylporphyrin)s (bis(OEP)–(M1–M2) and tris-(OEP)–(M1–M2–M3)) with d^8 transition-metal ions M(II) (M: M1, M2, and M3 = Ni or Pd or Pt) were synthesized by step-by-step and selective metallations of the respective free-bases (FB) with limited amounts of the metallation reagent. Metallation of tris(OEP)–(H_2–H_2–H_2) started in the central OEP ring, with the vinylene linkages of the product retaining the same (*E*,*E*)-configuration as those in FB. On the other hand, metallation of (*E*)-bis(OEP)–(H_2–H_2) afforded the corresponding (*E*)-bis(OEP)–(M1–M2) predominantly, while metallation of (*Z*)-bis(OEP)–(H_2–H_2) was accompanied by a ready isomerization of the vinylene linkage to afford each pair of (*E*)- and (*Z*)-isomeric complexes under the similar conditions. Electronic absorption spectra of tris(OEP)–(M1–M2–M3) proved to be affected especially by the central OEP–M2 ring and by the heavier metals more intensively, resulting in the largest splitting of the Soret band for the Ni–Pd–Pt complex. Examination of the oxidation potential E_1 values indicated that the electron-releasing abilities of tris(OEP)–(M1–M2–M3) are intensively reduced for the complex carrying at least two consecutive heavier metal OEP rings. In the case of bis(OEP)–(M1–M2), the (*E*)-isomeric series exhibited the reduction of the electron-releasing abilities regularly in order of the heavy metal complexes similarly to tris(OEP)–M, while the (*Z*)-isomeric series exhibited little dependence of the electron-releasing abilities upon the incorporated metals M.

Especially in the last decade, a great deal of effort has been given to the constructions of highly-ordered molecular architectures to understand the electronical communications between the various π-electronic constituents. Based on such results, electronic, electrochemical, and photoelectronic devices such as molecular switches, artificial photosynthesis reaction centers, molecular wires, and light-harvesting arrays have been designed so far. For the sake of such molecular architectures,[1] structurally defined porphyrin-based oligomers bridged with various linkages have appeared as promising candidates.

Previously we reported the synthesis of vinylene-bridged tris(octaethylporphyrin) (**13**: tris(OEP)–(H_2–H_2–H_2)),[2] by applying the synthetic methodology for the corresponding (*E*)-configurational bis(octaethylporphyrin) derivative (**5**: (*E*)-bis(OEP)–(H_2–H_2)).[3] The interaction between the constituent OEP rings through the vinylene linkage substantially influenced the electronic structure of mononucleic OEP–H_2 (**1**) to give rise to the new vibration bands reaching to the near-infrared wavelength region in the electronic absorption spectrum of **13**, proving that oligomerization of the OEP ring with the vinylene linkage enhances the electron-releasing ability and basicity of the OEP–H_2 ring regularly in order of **1** < **5** < **13**.[2,4] Subsequently, the uni-metallated bis- and tris(OEP)–M complexes (**5**—**16**) with the d^8 transition-metal ions M(II) (M: M1 = M2 = M3 = Ni or Pd or Pt) were synthesized for further investigation of the characteristic properties of this vinylene-bridged oligonucleic OEP system, since it is well known that the electronic structures of OEP-M (**1**—**4**) vary with the incorporated metal M. The d^8 transition-metal complexes of the porphyrin nucleus belong to a group of the hypsochromic type,[5] with respect to the absorption spectra, which is considered a significant property of such dyes as porphyrin in the molecular design for opto-electronic devices resistive to the visible light. Studies on their electronic absorption spectra and electrochemical properties proved that the interaction between the constituent OEP–M rings through the vinylene linkage is more intensive for tris(OEP)–M than for the corresponding (*E*)-bis(OEP)–M and yet more intensive for the Ni complex than for the Pd and Pt complexes in both bis- and tris(OEP)–M series.[6]

In continuation of our investigations on the properties of bis- and tris(OEP)–M in pursuit of the π-electronic constituent systems with various potential energy ladders,[1] a variety of the mixed complexes of the respective free-bases (FB) **5**, **9**, and **13** with the d^8 transition-metal ions M(II) (M: M1, M2, and M3 = Ni or Pd or Pt) were synthesized. In this paper, we wish to describe the synthesis of the title mixed complexes **17**—**41** (Chart 1) and to discuss their structural and electronic properties, as compared with those of **1**—**16**.

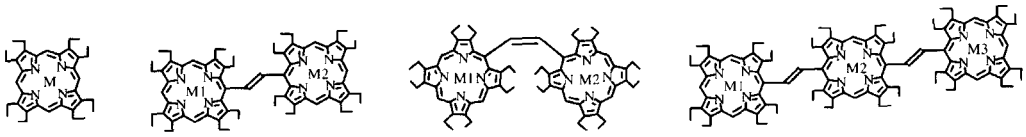

OEP-M

1: H_2
2: Ni
3: Pd
4: Pt

(*E*)-bis(OEP)-(M1-M2)

5: H_2-H_2
6: Ni-Ni
7: Pd-Pd
8: Pt-Pt
17: Ni-H_2
18: Pd-H_2
19: Pt-H_2
20: Ni-Pd
21: Ni-Pt
22: Pd-Pt

(*Z*)-bis(OEP)-(M1-M2)

9: H_2-H_2
10: Ni-Ni
11: Pd-Pd
12: Pt-Pt
23: Ni-H_2
24: Pd-H_2
25: Pt-H_2
26: Ni-Pd
27: Ni-Pt
28: Pd-Pt

tris(OEP)-(M1-M2-M3)

13: H_2-H_2-H_2
14: Ni-Ni-Ni
15: Pd-Pd-Pd
16: Pt-Pt-Pt
29: H_2-Ni-H_2
30: Ni-Ni-H_2
31: H_2-Pd-H_2
32: Pd-Pd-H_2
33: Ni-Pd-H_2
34: Pd-Ni-H_2
35: Ni-Ni-Pd
36: Ni-Ni-Pt
37: Ni-Pd-Ni
38: Ni-Pd-Pd
39: Ni-Pd-Pt
40: Pd-Ni-Pd
41: Pd-Ni-Pt

Chart 1.

Results and Discussion

Synthesis. Syntheses of the uni-metallated complexes of bis(OEP)–M (**6**—**8** and **10**—**12**) and tris(OEP)–M (**14**—**16**) were previously performed by the reaction of FB **5**[3] and **13**[2] with large excessive amounts of the metallation reagents, under the slightly modified reaction conditions for the preparation of **2**—**4** from **1**.[7] Probably due to such particular conditions using a larger amount of the metallation reagents and taking a somewhat longer reaction time than usual for OEP–M, metallation of **5** was accompanied by an isomerization of the vinylene linkage to afford a considerable amount of the (*Z*)-bis(OEP)–M complex together with the main product of the (*E*)-isomer.[6] Therefore, in order to avoid more intricacy of the products and to attain a reliability for the incorporation of each metal into the specific FB ring, the syntheses of the title mixed complexes **17**—**41** were carried out by the step-by-step and selective metallations of the respective FB rings with very limited amounts of the metallation reagents and within fairly short reaction times, except for the final complexation stage, as shown in Schemes 1 and 2.

(I) (*E*)- and (*Z*)-Bis(OEP)–(M1–M2): In the case of (*E*)-isomeric series of the monometallated complexes described as M1–H_2, nickelation of **5** with one molar equivalent of the acetate salt ($Ni(OAc)_2 \cdot 4H_2O$) in a mixture of chloroform ($CHCl_3$) and methanol (MeOH) readily took place to afford the Ni–H_2 complex **17** in 32% yield. Although these conditions did not induce any isomerization of the vinylene linkage at all, as expected, the Ni–Ni complex **6**[3,6] was also obtained in 12% yield based on $Ni(OAc)_2 \cdot 4H_2O$, together with 31% recovery of **5**. Palladation of **5** also exhibited a similar result for the nickelation, to afford the Pd–H_2 complex **18** (37%) as the main product together with the Pd–Pd complex **7**[6] (20% based on $Pd(OAc)_2$) and FB **5** (32%). The fact that the dimetallated product was obtained under these controlled reaction conditions suggests that the first-metallated OEP–M1 ring enhances the acidity of NH proton belonging to the neighboring FB ring (also see Section II and Experimental). On the other hand, the platination of FB **5** to the Pt–H_2 complex **19** was very hard under the ordinary conditions; the same case was found with **5** to the uni-platinated complex **8**.[6] The fairly low reactivity of **5** to platination being taken into consideration, treatment of **5** with 5 molar

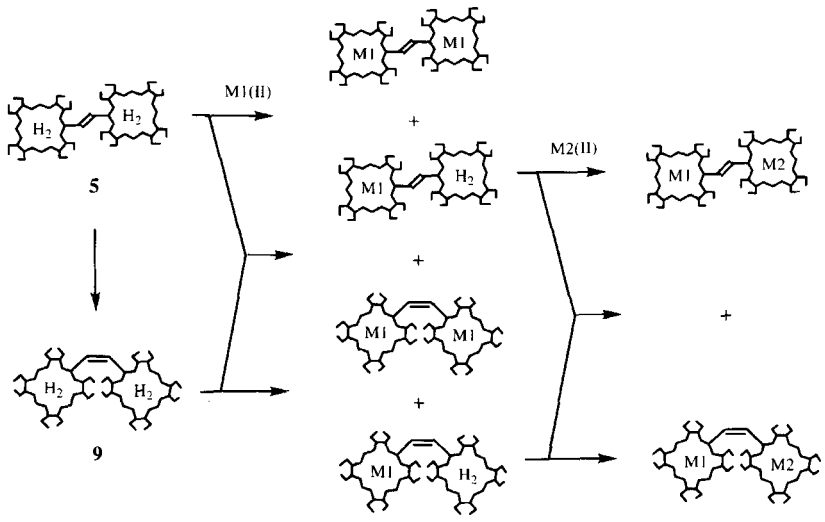

Scheme 1.

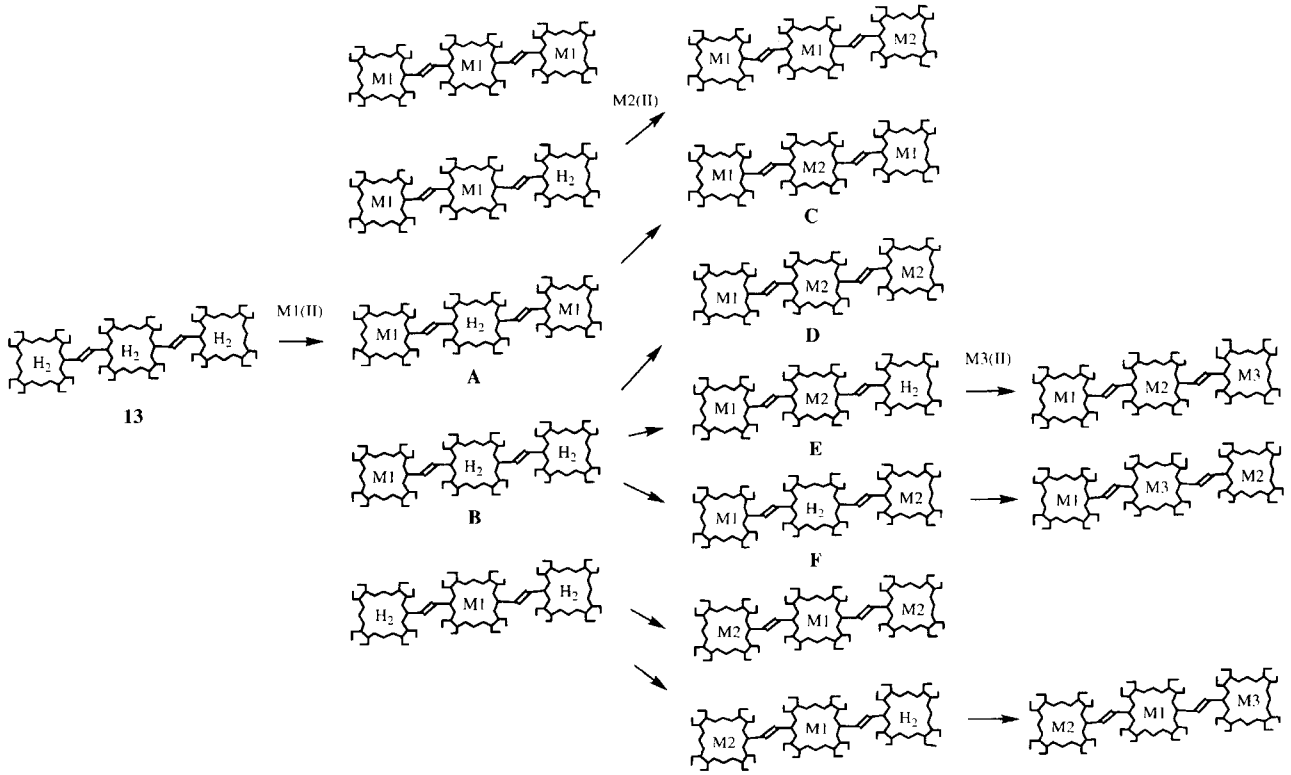

Scheme 2.

equivalent of platinum(II) chloride ($PtCl_2$) in a mixture of $CHCl_3$ and acetic acid (AcOH) was found to be convenient for **19**, but the yield of **19** was still as low as 10% along with 40% recovery of **5**. Another trial of the preparation of **19** using 4 molar equivalents of $Pt(acac)_2$ to **5** in AcOH resulted in increasing the yield of **19** to 19% and in decreasing the unreacted quantity of **5** (19%). In this case, however, not only further platination of **19** but also isomerization of the vinylene linkage took place to afford a fairly complicated mixture containing the Pt–Pt complex **8** (7.4%) and the (*Z*)-isomeric Pt–H_2 complex (**25**: 17%, see below) and FB (**9**:[8] 10%).

The M1–H_2 complexes **17**—**19** thus obtained were found to lower their solubilities extremely in ordinary organic solvents, as compared with that of FB **5**, in order of the heavy metal complex M1: Ni > Pd ≫ Pt. Therefore, among possible combinations of the substrates with the metallation conditions for the M1–M2 complex, the more soluble M1–H_2 complex was employed as the intermediate FB material for the next (final) complexation. Thus, palladation of **17** with $Pd(OAc)_2$ afforded the Ni–Pd complex **20** in 90% yield. Platination of **17** with $PtCl_2$ gave the Ni–Pt complex **21** in 33% yield together with 35% recovery of **17**. Platination of **18** with $PtCl_2$ afforded the desired Pd–Pt complex **22** (32%) in almost the same yield as that in the platination of **17** to **21**, but **18** was not recovered at all and instead a considerable amount of insoluble material containing a trace of the (*Z*)-isomeric Pd–Pt complex **28** (see below) was formed.

In the case of the (*Z*)-bis(OEP)-(M1–M2) complexes, the FB **9** prepared by an acid-catalyzed isomerization of **5** according to the reported procedure[8] was metallated under the respective conditions, similarly for the corresponding (*E*)-isomers. However, the results were rather different between these (*E*)- and (*Z*)-isomeric series here and there. Nickelation of **9** with one molar equivalent of $Ni(OAc)_2 \cdot 4H_2O$ gave the Ni–H_2 complex **23** in 45% yield together with a trace of the (*Z*)- and (*E*)-isomeric Ni–Ni complexes (**6** and **10**[6]), the (*E*)-isomeric Ni–H_2 complex **17** (6.3%), and 14% recovery of **9**. Similarly, palladation of **9** with one molar equivalent of $Pd(OAc)_2$ afforded the Pd–H_2 complex **24** in 39% yield together with a trace of the (*E*)- and (*Z*)-isomeric Pd–Pd complexes (**7** and **11**[6]), the (*E*)-isomeric Pd-H_2 complex **18** (7.3%), and 36% recovery of **9**. Platination of **9** with 4 molar equivalents of $Pt(acac)_2$ also showed a similar result to the other metallations, affording the Pt–H_2 complex **25** in 18% yield as well as traces of the (*E*)- and (*Z*)-isomeric Pt–Pt complexes (**8** and **12**[6]), the (*E*)-isomeric Pt–H_2 complex **19** (10%), and 36% recovery of **9**.

Then, syntheses of the mixed M1–M2 complexes **26**—**28** were carried out by metallations of all the M1–H_2 complexes **23**—**25**, because of their much higher solubilities as compared with the corresponding (*E*)-isomeric M1–H_2 complexes. Palladation of **23** with $Pd(OAc)_2$ afforded the desired Ni–Pd complex **26** in 86% yield together with the (*E*)-isomer **20** (12%). For the synthesis of the Ni–Pt complex **27**, both platination of **23** and nickelation of **25** were examined under ordinary conditions. The former afforded only a trace of the (*Z*)- and (*E*)-isomeric Ni–Pt complexes **21** and **27** but, to be surprised, the latter was not accompanied by any isomerization of the vinylene linkage at all, affording the desired complex **27** exclusively and quantitatively. A similar trend was also observed for the synthesis of the Pd–Pt complex

28. Platination of **24** by the usual way produced only a trace of the (*Z*)- and (*E*)-isomeric Pd–Pt complexes **22** and **28**, while palladation of **25** afforded the desired product **28** in 85% yield together with the (*E*)-isomer **22** (11%).

(II) Tris(OEP)–(M1–M2–M3): Based on the fact that the acidity of NH protons belonging to the central OEP ring of FB **13** proved to be higher than that of NH protons belonging to the outer OEP rings by the H–D exchange experiment,[2] syntheses of the mixed metal complexes **29**—**41** were planned initially by carrying out the selective metallation of the central OEP ring, followed by metallations of the rest OEP rings step by step, as shown in Scheme 2. Nickelation of **13** with 1 molar equivalent of $Ni(OAc)_2 \cdot 4H_2O$ in a mixture of $CHCl_3$ and MeOH (5 : 1) afforded a mixture of the mono- (**29**), di- (**30**), and trinickelated (**14**) complexes in 32%, 24%, and less than 1 % yields (all based on $Ni(OAc)_2 \cdot 4H_2O$), respectively, together with 30% recovery of **13**. In this mixture, any other products more than these three complexes were not found, except for a small amount of the insoluble material. By means of ^{1}H NMR spectral measurements, the signals due to NH protons from the central OEP ring of **13** were found to disappear completely in the spectra of all the metallated products, apparently indicating no possibilities of the products such as **A** and **B** but the structure of the mononickelated product to be the H_2–Ni–H_2 complex **29** and the structure of the dinickelated product to be the Ni–Ni–H_2 complex **30**. From these results, it can be concluded that the first nickelation of **13** takes place in the central OEP ring exclusively and that the already nickelated OEP ring accelerates the further metallation of the neighboring FB ring. Similarly, palladation of **13** with 1 molar equivalent of $Pd(OAc)_2$ in the same medium as for the nickelation readily occurred to give a mixture of the H_2–Pd–H_2 (**31**), Pd–Pd–H_2 (**32**), and Pd–Pd–Pd (**15**) complexes in 19%, 39%, and 22% yields (all based on $Pd(OAc)_2$), respectively, together with 10% recovery of **13**. This result apparently indicates that the incorporated metal effect on the acceleration of the further metallation is greater for the palladation than for the nickelation.

With respect to the second metallation products summarized in a categorical sequence (Scheme 2), the structures such as **C**, **D**, **E**, and **F** formed through the postulated courses via unfeasible compounds **A** and **B** could be excluded. The difference in reactivity of **13** between nickelation, palladation, and platination being taken into consideration, syntheses of the mixed complexes **33**—**41** were performed by treatment of **29**—**32** with the corresponding metal reagents under the milder reaction conditions, unless otherwise stated. Thus, the Ni–Pd–H_2 complex **33** was prepared in 41% yield by the nickelation of **31**, under the conditions in which the substance **31** was recovered in 20% yield. Similarly, the Pd–Ni–H_2 complex **34**, an isomer of **33**, was prepared in 30% yield by the palladation of **29**, under the conditions in which the substance **29** was recovered in 43% yield. Under these nickelation and palladation conditions, the symmetrical Ni–Pd–Ni (**37**; 21% from **31**) and Pd–Ni–Pd complexes (**40**; a trace from **29**) were also obtained, both of which could be alternatively prepared in the respective yields of 60 and 70%, when treated with an excessive amount of each reagent (see Experimental). Then, the palladation of **30** with a large excess of $Pd(OAc)_2$ afforded the Ni–Ni–Pd complex **35** in 80% yield. On the other hand, the platination of **30** afforded the Ni–Ni–Pt complex **36**, but the yield of **36** was only 26% together with 33% recovery of **30**, in spite of the optimum conditions for platination using a large excess of $PtCl_2$ in AcOH.[7b] Synthesis of the Ni–Pd–Pd complex **38** was performed in 75% yield by the nickelation of **32**. Finally, the platination of **33** and **34** afforded the isomeric Ni–Pd–Pt (**39**)[9] and Pd–Ni–Pt (**41**) complexes in 32 and 29% yields, respectively, which can be regarded as ternary mixed OEP–M arrays.

However, the synthesis of the last ternary isomer, the Ni–Pt–Pd complex (**42**), was abandoned, because of several disadvantages of the intermediate H_2–Pt–H_2 complex **43** (Chart 2). Although the formation of **43** could be ascertained on the bases of MS and ^{1}H NMR measurements, (i) the precursor **43** was hard to isolate from the mixture of the Pt–Pt–Pt (**16**) and Pt–Pt–H_2 (**44**) complexes, (ii) the yield of **43** was extremely low even under the optimum platination conditions, and (iii) the solubility of **43** was too low to achieve its full characterization.

^{1}H NMR Spectra. ^{1}H NMR spectra of all the metal complexes as well as FB **1**, **5**, **9**, and **13** (Chart 3) were measured in $CDCl_3$ at 25 °C, unless otherwise stated. Chemical shifts due to the *meso*, vinylene, and NH protons of the selected complexes are summarized for discussions in Charts 4, 5, and 6.

(III) (*E*)- and (*Z*)-Bis(OEP)–(M1–M2): From the previous studies on ^{1}H NMR spectral behaviors of the uni-metallated bis(OEP)–M complexes (**6**—**8** and **10**—**12**), the following three conclusions were derived; (i) the diamagnetic ring current effect of the constituent OEP–M ring decreases in the same order of M = $H_2 \approx$ Pd > Pt $\gg$ Ni as that of OEP–M (**1**—**4**), (ii) the molecular planarity through the vinylene linkage in (*E*)-bis(OEP)–M deforms into a stairway-like structure to more extent for the heavier metal complex, and (iii) the dihedral angle between two faced OEP–M rings in (*Z*)-bis(OEP)–M is smaller for the heavier metal complexes.[6] As can be seen in Charts 4 and 5, the results from the mixed bis(OEP)–(M1–M2) complexes (**17**—**28**) seem to support the previous findings and to show the validity in their qualitative additivities to a considerable extent, for construing the structural changes arised from the unsymmetrical metallations of FB **5** and **9**.

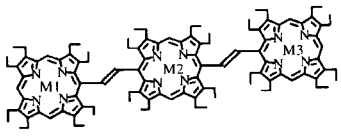

tris(OEP)-(M1-M2-M3)

42: Ni-Pt-Pd
43: H_2-Pt-H_2
44: Pt-Pt-H_2

Chart 2.

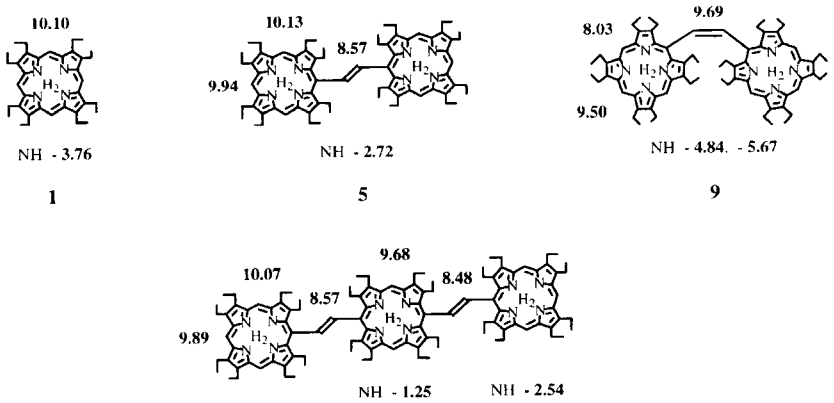

Chart 3.

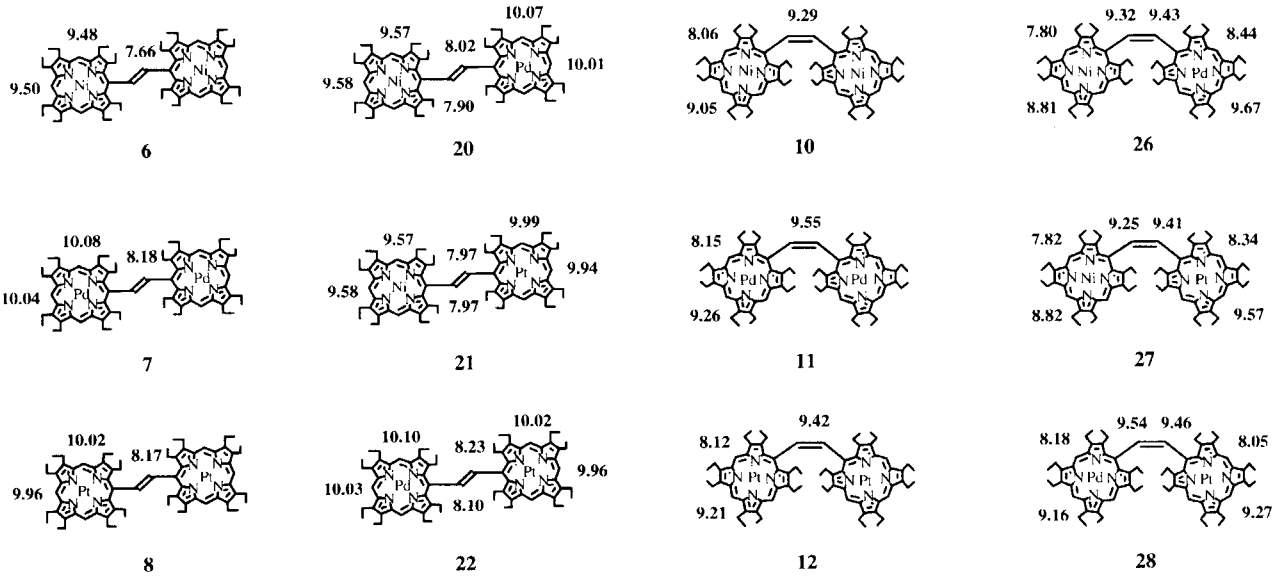

Chart 4.

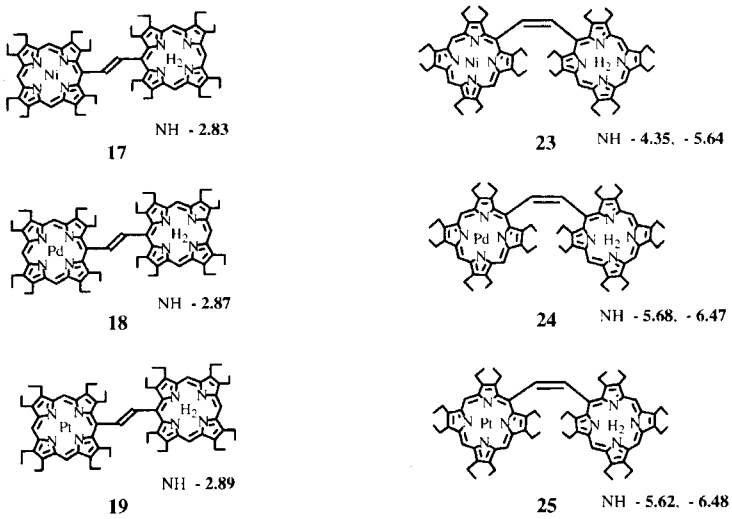

Chart 5.

It is pointed out that in the case of an (*E*)-bis-(OEP)–(Ni–M2) series, both meso protons of the OEP–Ni ring and vinylene protons nearby the OEP–Ni ring of **20** and **21** appear at the lower fields than the corresponding protons of the uni-metallated Ni-complex **6**. On the other hand, such meso and vinylene protons belonging to the OEP–Pd

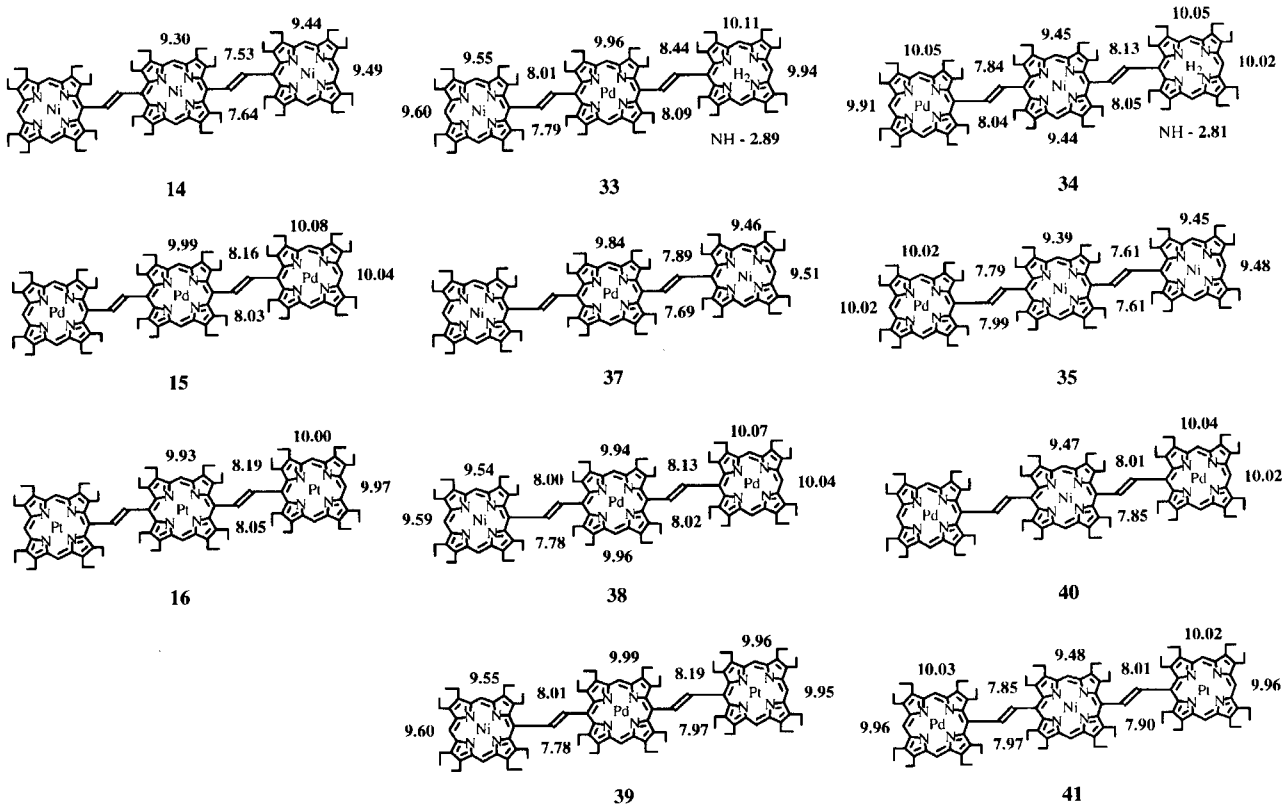

Chart 6.

or OEP–Pt ring of **20** or **21** appear at the higher fields than the corresponding protons of the uni-metallated Pd (**7**) or Pt complex (**8**). As concluded from the studies of the uni-metallated bis-(OEP)–M,[6] these results might be interpreted by anisotropic effect changes from these OEP–Ni and OEP–M2 rings, reflecting not only the smaller diamagnetic ring current of the OEP–Ni ring but also the conformational changes of the OEP–Ni and OEP–M2 rings around the vinylene linkage, where these meso and vinylene protons belonging to the OEP–Ni ring are affected by the farther OEP–M2 ring more intensively.

Furthermore, it is clearly shown that oligomerization of FB **1** with the (*E*)-vinylene linkage at the *meso* position induces the NH protons to shift to the low field by more than 1 ppm, though the reason for such a large low-field shift of the NH protons of **5** needs further study. However, since the *meso* protons of **1** and **5** resonate at almost the same field, this result could not be simply due to the reduction of their ring currents and/or from the inductive effect of the vinylene linkage, but must rather be induced by the loss of the molecular symmetry. In relation with this expectation, it is curious to note that NH protons of the M–H_2 complexes (**5** and **17**—**19**) shifted to the high field regularly in order of the heavy metal; M = H_2 < Ni < Pd < Pt, though within a small range, also suggesting the different anisotropic effects from the respective OEP–M rings on the chemical shifts for NH protons of the neighboring FB ring.

The (*E*)-bis(OEP)–M complexes would be stabilized by changing their structural properties in two ways: one is due to the back-donation interaction of the incorporated metal M into the OEP ring; the other is due to the resonance effect from the OEP–M ring by taking part in a full-conjugation through the vinylene linkage. The resonance stabilization is essentially important for the stability of the OEP–M rings but, in this case, it causes the severe steric repulsion between the vinylene linkage and the peripheral ethyl substituents, since the respective OEP–M rings are to be in a planar conformation throughout the vinylene linkage. Therefore, when the back-bonding interaction overcomes such resonance effect, the whole molecule would twist into a stairway-like conformation to achieve more stabilization. Although such stairway-like structures of the M1–M2 complexes can be expected to distort unsymmetrically about the vinylene linkage, the magnitude of deformation of each OEP–M ring from the molecular plane throughout the vinylene linkage would be greater for the heavier metal OEP–M ring, since the back-bonding interaction is known to be more intensive for the heavier d^8 metal complexes, thus quite eminent for OEP–Pt **4**,[5] as shown in Fig. 1. In other words, the heavier metal

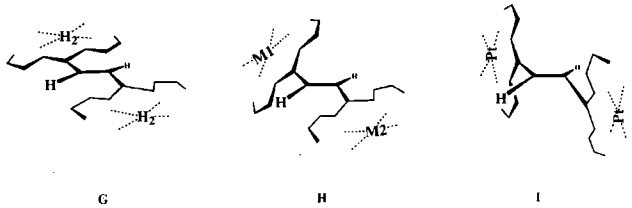

Fig. 1. Geometrical changes for the M1–M2 complexes from the most planar conformation **G** of **5** to the least planar conformation **I** of **8**.

OEP–M ring is more liable to isolate electronically. The fact that the up-field shift was observed for the vinylene proton nearby the heavier metal OEP ring apparently supports such structural changes, as is also observed for the uni-metallated complexes,[6] indicating that the constituent OEP–M1 and OEP–M2 rings exist in the molecular conformation **H** with particular distortion angles for each OEP–M ring between **G** for the most planar FB **5** and **I** for the least planar Pt–Pt complex **8** (also see Section IV).

The spectral behavior of the mixed (*Z*)-bis(OEP)–(Ni–M2) (**26** and **27**) was completely reversed with that of the corresponding (*E*)-bis(OEP)–(Ni–M2). Meso protons of the OEP–Ni rings in **26** and **27** appeared at the much higher fields than the corresponding protons of the uni-metallated Ni complex **10**, while *meso* protons of the OEP–Pd and OEP–Pt rings appeared at the lower fields than the corresponding protons of the uni-metallated Pd and Pt complexes **11** and **12**. It is also proved that vinylene protons of all the metal complexes appear at the higher fields than those of FB **9** and that each vinylene proton nearby the constituent OEP–M1 or OEP–M2 ring resonates at the very similar region to the corresponding protons of the respective uni-metallated complex. These results might be attributed to the different dihedral angles between two faced OEP–M1 and OEP–M2 rings, in addition to the ring current effect of the OEP–Ni ring being smaller than that of the OEP–Pd and OEP–Pt rings. The larger dihedral angle would make the distance between the constituent OEP–M rings longer and oppositely the distance between two vicinal vinylene protons shorter, where the anisotropic effect from the OEP–M1 ring to the meso protons of the OEP–M2 ring (vice versa) decreases and oppositely the steric compression between two vinylene protons increases. In this respect, it could be derived that all the metal complexes possess smaller dihedral angles than FB **9** through an attractive interaction between the faced OEP–M1 and OEP–M2 rings more or less, since the respective OEP–M of the uni-metallated complex retains its inherent diamagnetic ring current.[6]

It is interesting to note that NH protons in the (*Z*)-isomeric M1–H_2 complexes (**23**—**25**) as well as FB **9** exhibited two different signals, unlike those in the corresponding (*E*)-isomers, both of which appeared at the further high fields than those of the corresponding (*E*)-isomers (Chart 5). Mean values of chemical shifts of the NH protons became larger in negative value in the order of M1 = Ni < H_2 ≪ Pd ≈ Pt over a wide range, as contrasted with those for the (*E*)-isomeric series. These results apparently indicate that the transannular interaction induces the tight fixation of the NH bonds in the FB ring, in addition to the hard rotation of each OEP ring around the vinylene linkage, and that the anisotropic effect from the OEP–M1 ring affects straight the confronted NH protons. In particular, since the magnitude of the diamagnetic ring current of OEP–H_2 (**1**) is known to be almost the same as that of OEP–Pd (**3**),[10] such a high field shift of NH protons in the Pd–H_2 complex **24** shows an intensive interaction between the constituent OEP–Pd and OEP–H_2 rings, also indicating a much smaller dihedral angle between two faced OEP rings for **24** than for FB **9**. This is also the same case as with the Pt–H_2 complex **25**.

(IV) Tris(OEP)–(M1–M2–M3): Similar to the (*E*)-bis(OEP)–M complexes, the uni-metallated tris(OEP)–M complexes (**14**—**16**) were previously proved to exhibit their structural changes from the most planar conformation of FB **13** into the stairway-like conformation around the vinylene linkage to a greater extent by palladation and platination than by nickelation.[6] In other words, it might be concluded that tris(OEP)–M possesses a conformational structure simply extended from that of the corresponding (*E*)-bis(OEP)–M, as illustrated in Fig. 2. These structural changes result especially in the high field shift of vinylene protons due to an anisotropic effect from the adjacent OEP–M, since each OEP–M ring in the tris(OEP)–M complex scarcely reduces its inherent diamagnetic ring current. Vinylene protons of the Pd complex **15**, for example, appear at the fields higher by 0.3—0.5 ppm from those of **13**.[11] This trend was observed even at each metallation step of **13** as well. In the case of the Pd–Pd–H_2 complex (**32**), three of four vinylene protons resonated at the high field region from the last one, thus providing some crucial information on the structural assignment of the already metallated OEP ring of **13**. However, the reason why vinylene protons for the Ni complexes (**14**, **29**, and **30**) also appear at such high fields as those for the Pd and Pt complexes can not be attributed to similar conformational changes, but rather to the small ring current of OEP–Ni ring itself (also see Section VI).[6] On the basis of these peculiar features of the uni-metallated (*E*)-bis- and tris(OEP)–M complexes, including their partially metallated ones as well as H–H COSY experiments, the assignments of all the meso and vinylene protons of the mixed complexes were unambiguously performed.

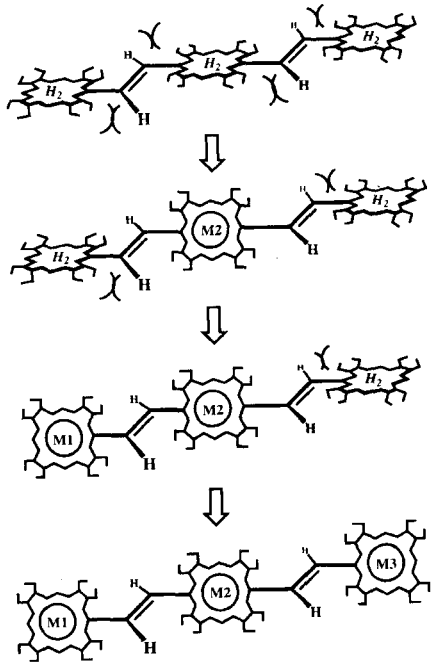

Fig. 2. Conformational changes of the M1–M2–M3 complexes on metallations of the most planar FB **13**.

Two isomeric series of the Ni–Pd–M3 (**33**, **37**, **38**, and **39**) and Pd–Ni–M3 complexes (**34**, **35**, **40**, and **41**) as well as the uni-metallated tris(OEP)–M (**14**, **15**, and **16**) are shown in Chart 6. *Meso* protons of the respective OEP rings in the mixed complexes exhibited fairly similar chemical shifts to those of the corresponding OEP rings in the uni-metallated complexes, indicating that each OEP ring retains its inherent ring current to a considerable extent even in the mixed complexes. Vinylene protons nearby the OEP–M3 ring also varied in parallel with those in the uni-metallated tris(OEP)–M in both mixed complex series, but the respective chemical shift differences of these vinylene protons between the mixed and uni-metallated complexes are greater in the latter Pd–Ni–M3 series, resulting in more up-field shift for the latter isomers than for the corresponding former isomers. On the other hand, NH protons of the latter Pd–Ni–H_2 complex **34** appeared at the lower field than those of the former Ni–Pd–H_2 isomer **33**. These results could be substantially ascribed to their structural changes around the vinylene linkage from the most planar conformation of FB **13** induced by the respective metallations, similarly to bis(OEP)–(M1–M2), in addition to the small ring current of the OEP–Ni complex **2**. Although the two ternary M1–M2–M3 complexes (**39** and **41**) exhibited very similar spectra to each other in both signal patterns and chemical shifts, it is obvious that the *meso* proton signals of the OEP–Ni ring at around 9.5 ppm are two for **39** and one for **41**. Reflecting the small ring current of the OEP–Ni ring in the central position of the M1–M2–M3 complex, *meso* protons of the OEP–Pd and OEP–Pt rings of **41** exhibited the low field shifts, as compared with the corresponding protons in **39**.

The complexes **35** and **37** carrying two OEP–Ni rings showed a curious discriminative behavior in their signal shapes. The Ni–Pd–Ni complex **37** exhibited very sharp signals for all meso and vinylene protons, while the Ni–Ni–Pd complex **35** exhibited much broader signals for all of them even at 50 °C, as compared with the Ni–Ni–Ni complex **14**. This result suggests that the atrop-isomerism around the central OEP–M ring in the tris(OEP)–M complex, where the coalescence between the two atrop-isomers is deduced to occur at around room temperature,[6,12] is essentially induced by the two consecutive OEP–Ni rings and is severely retarded by the heavier metal incorporated in the last OEP ring. In other words, the activation energy for interconversion between the atrop-isomers is indicated to be greater in the heavier metal complex of Ni–Ni–M type, in accordance with the behaviors in the conformational change to the more stairway-like structure for the heavier metal complex of M–M–M type.

Electronic Absorption Spectra. Electronic absorption spectra of all the metal complexes were measured in $CHCl_3$ at 25 °C, unless otherwise stated. The spectra for pairs of the (*E*)- and (*Z*)-bis(OEP)–(Ni–Ni) (**6** and **10**), –(Ni–Pd) (**20** and **26**), and –(Pd–Pd) (**7** and **11**) complexes, a series of tris(OEP)–(Ni–Ni–M3) complexes (**14**, **35**, and **36**), and a series of tris(OEP)–(Ni–Pd–M3) complexes (**33**, **37**, **38**, and **39**) are shown in Figs. 3, 4, and 5, respectively.

(V) (*E*)- and (*Z*)-Bis(OEP)–(M1–M2): Reflecting the more planar conformation throughout the vinylene linkage, the Ni–Ni complex **6** exhibits a weak absorption band (WAB) tailing up to 800 nm, as is deduced from the conclusion of ^{1}H NMR spectra (Fig. 3). The Pd–Pd complex **7**, however, did not exhibit such a characteristic band of the π-electronic

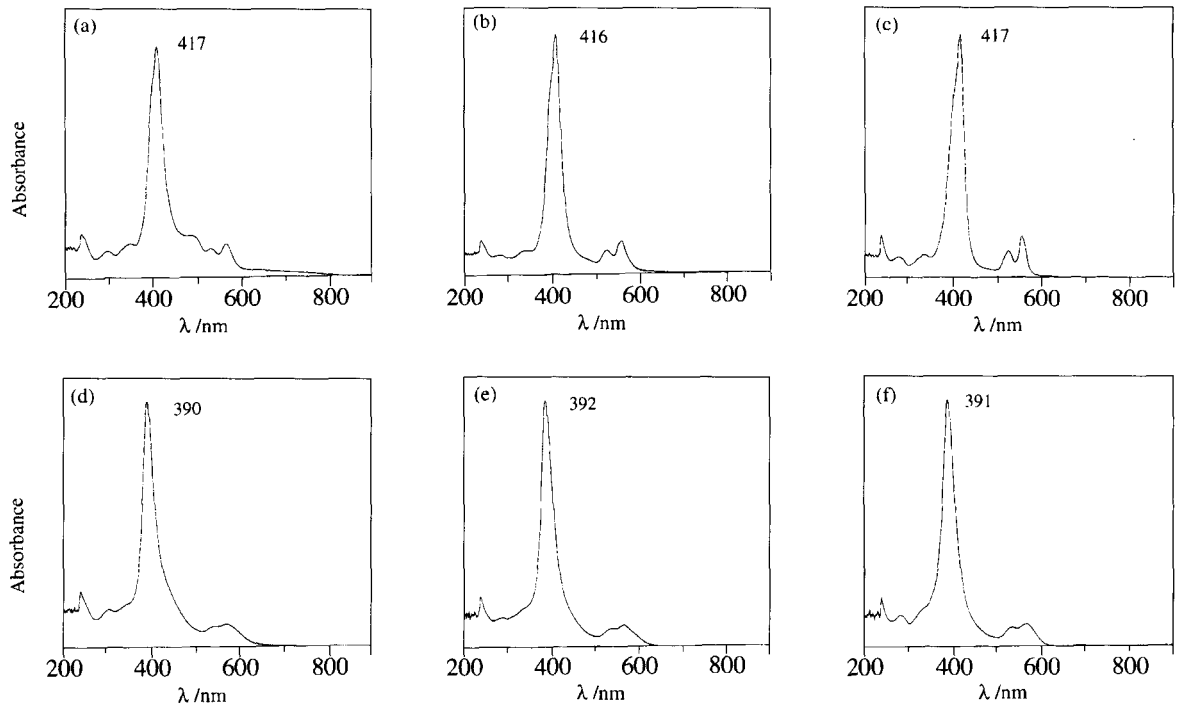

Fig. 3. Electronic absorption spectra of (*E*)- and (*Z*)-isomeric pairs of the bis(OEP)–(Ni–Ni), –(Ni–Pd), and –(Pd–Pd) complexes; (a) for **6**, (b) for **20**, (c) for **7**, (d) for **10**, (e) for **26**, (f) for **11**.

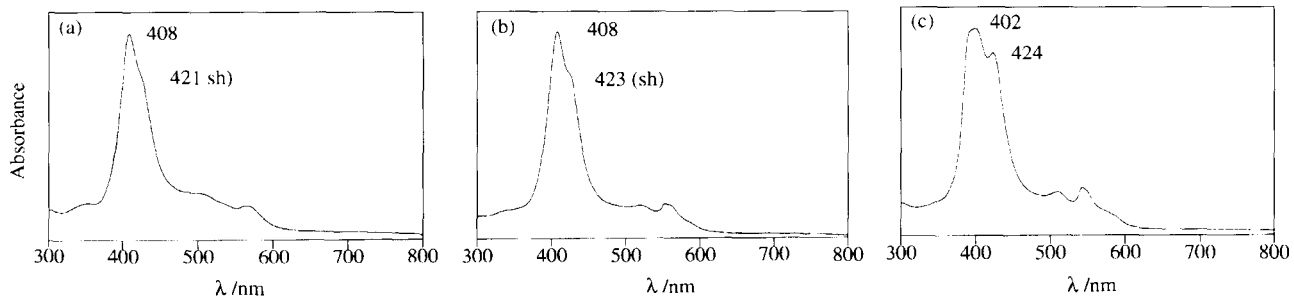

Fig. 4. Electronic absorption spectra of the tris(OEP)-(Ni-Ni-M3) complexes; (a) for **14**, (b) for **35**, (c) for **36**.

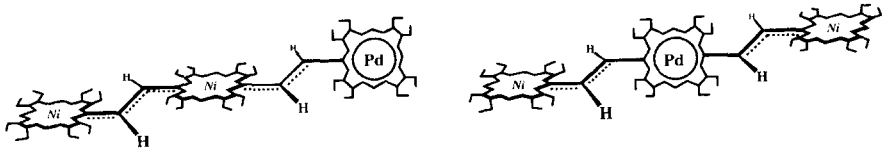

35 37

Fig. 5. Conformational difference between the Ni–Ni–Pd (**35**) and Ni–Pd–Ni (**37**) complexes, in which the heavier metal OEP ring brings the π-electronic conjugation planarity to destruction into a partial stairway-like conformation.

interaction between the constituent OEP rings at all to afford almost the same absorption curve as that of the mononucleic OEP–Pd complex **3**. This result suggests that **7** exists in a stairway-like conformation around the vinylene linkage, where two OEP–Pd rings are electronically isolated. In the case of the mixed Ni–Pd complex **20**, the spectrum is rather comparable to that of **7** with WAB almost disappearing, indicating that the electronic structural property is affected more severely by the heavier metal. On the other hand, the Soret bands exhibited little difference among these complexes **6**, **7**, and **20**, in spite of a remarkable difference in the molecular planarity between them, to afford the maxima for all of them at around 417 nm. Since the value of 417 nm corresponds to the more than 20 nm bathochromic shift from the maxima of the respective Soret bands for OEP–Ni (**2**) and OEP–Pd (**3**),[6,7] this suggests a through-space interaction between two metallated OEP rings existing in the more stairway-like conformation of **20**, with the electronic structures of **2** and **3** almost unchanged but with their transition energy gaps only reduced.

In contrast with the results of (*E*)-bis(OEP)-(M1–M2), the absorption spectra of (*Z*)-isomers exhibited no particular difference between the Ni–Ni (**10**), Ni–Pd (**26**), and Pd–Pd (**11**) complexes. All exhibited the hypsochromic shift of the Soret bands by ca. 25 nm from the corresponding (*E*)-isomeric ones, resulting in giving almost the same maxima as those of the corresponding OEP–M complexes (**2** and **3**), together with their intensities increasing. As also observed in a pair of (*E*)- and (*Z*)-bis(OEP)-(Pt–Pt) **8** and **12**,[6] the Q bands of all these (*Z*)-isomeric complexes are much broader than those of both corresponding (*E*)-bis(OEP)–M and OEP–M. These facts indicate a transannular interaction between the constituent OEP–M rings in a (*Z*)-isomeric series, which arises most likely from the exciton coupling due to the face-to-face orientation of the respective OEP–M rings,[13] though these OEP–M rings are liable to isolate electronically to be like OEP–M.

(VI) Tris(OEP)-(M1–M2–M3): As can be seen in Fig. 4, WAB is more outstanding for the Q-bands of the Ni–Ni–Ni (**14**), Ni–Ni–Pd (**35**), and Ni–Ni–Pt (**36**) complexes tailing up to 1100 nm, which is of characteristic for the mutual interactions between the three OEP rings throughout the vinylene linkage.[2] With respect to the Soret bands, it is shown that two absorption bands clearly appear, as the heavier metals are incorporated into the Ni–Ni–H_2 complex **30**. The overall spectra of the Ni–Ni–M3 complexes, however, are notably broad. These results would be attributed to the structural changes induced especially by the metal incorporated into the central OEP ring, reflecting a synergistic effect from the resonance stabilization of the OEP–M rings through the vinylene linkage and from the through-space interaction between the constituent OEP–M rings. The Ni–Ni–Pd complex **35**, for example, is expected to be in a particular structure from the ^{1}H NMR study, where two consecutive OEP–Ni rings exist in a more conjugation planar conformation throughout the vinylene linkages but two consecutive OEP–Ni and OEP–Pt rings exist in a more twisted conformation about the vinylene linkage, so-called, a partial stairway-like conformation (Fig. 5). Contrary to such spectral behaviors of the Ni–Ni–M3 complexes, the Ni–Pd–M3 complexes seem to reduce the resonance interaction between the three OEP rings remarkably (Fig. 6). For example, such a weak but long absorption tail dramatically disappeared in the spectrum of the Ni–Pd–Ni complex **37**, an isomer of **35**, to afford the fairly simple Q bands with two maxima. Similarly, it is proved that **38** and **39** possess no absorptions in the wavelength region longer than 700 nm, affording the quite sharp absorption curves. Therefore, it is concluded that the interaction between the constituent OEP rings is severely affected by the heavy metal of the central OEP–M2 ring, as illustrated in Fig. 5. This reflects on their color appearances in solid state as well, giving the black purple color to **35** and **36** similar to **14**, while giving the shining reddish purple color to **37** and **38**.

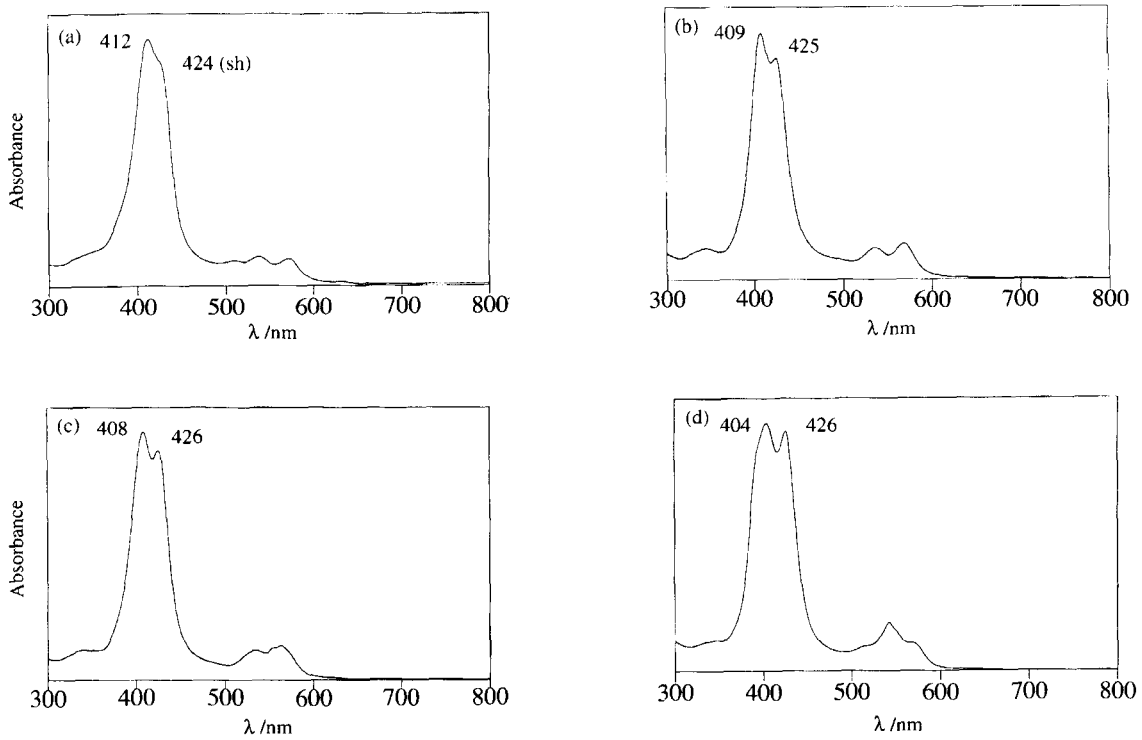

Fig. 6. Electronic absorption spectra of the tris(OEP)–(Ni–Pd–M3) complexes; (a) for **33**, (b) for **37**, (c) for **38**, (d) for **39**.

The heavier metals also induced the splitting of the Soret bands of the Ni–Pd–M3 complexes into two main bands. Interestingly, the longer wavelength bands of the Soret bands were almost unchanged in all complexes to give the absorptions at around 425 nm, while the shorter wavelength ones exhibited the hypsochromic shift in the order of M3 = H_2 < Ni ≈ Pd < Pt, resulting in the largest splitting ($\Delta\lambda$ = 22 nm) of the Soret band for the Ni–Pd–Pt complex **39**.[9] A similar trend is also observed in a series of the mono-, di-, and tri-metallated Pd complexes. As the Pd metal is incorporated one by one, the color appearances of the complexes become more bright in order of **31** < **32** < **15**, among which the Pd–Pd–Pd complex **15** gave no absorptions in a region of more than 600 nm and gave the sharp Soret bands with a clear splitting ($\Delta\lambda$ = 18 nm).[11] These results apparently indicate that incorporation of the heavier metal induces the molecular planarity of tris(OEP)–M to twist about the vinylene linkage into a stairway-like conformation more intensively, resulting in an interruption of the π-electronic conjugation between the constituent OEP rings, consistent with the results from the ^{1}H NMR studies (see Fig. 2).

Cyclic Voltammetry. Electrochemical properties of the mixed complexes **17**—**41** were examined by means of cyclic voltammetry, under the same conditions for the uni-metallated complexes **1**—**16** (see Experimental).[6] In the case of a series of OEP–M, the oxidation is well known to proceed via two one-electron transfer processes to afford the corresponding dicationic species and the products at the first oxidation stage, radical cations, were formed at the respective potentials ($E_1^{1/2}$; 0.94 V for **1**, 0.86 V for **2**, 1.04 V for **3**, and 1.09 V for **4**) in order of the ionization tendency of M,[6,14] indicating the highest electron-releasing ability of the OEP–Ni complex **2**. The electron-releasing abilities of the complexes were estimated from the first half-wave oxidation potential E_1 values in the first scanning voltammograms, since some of them which include the FB rings afforded the irreversible voltammograms, probably due to some electrochemically induced reactions such as geometrical isomerization of the vinylene linkage[15] and polymerization. Figure 7 shows the changes of the E_1 values for the (*E*)- and (*Z*)-bis(OEP)–(M1–M2) complexes and Fig. 8 for the tris(OEP)–(M1–M2–M3) complexes.

(VII) (*E*)- and (*Z*)-Bis(OEP)–(M1–M2): It is proved that all the bis(OEP)–(M1–M2) complexes were oxidized via three or four electron transfer processes to the final products, which might be assigned to be the corresponding bis(dicationic) species.[6] As shown in Fig. 7(a), the electron-releasing abilities of the (*E*)-isomeric series decrease in order of the heavy metal M2, apparently exhibiting the highest for the Ni–H_2 complex **17** and the lowest for the Pt–Pt complex **8**. As was concluded from the ^{1}H NMR and electronic absorption spectral studies, the electron-releasing abilities of the (*E*)-bis(OEP)–(M1–M2) complexes also exhibited the parallel correlation with the degrees of the molecular planarity throughout the vinylene linkage, resulting in the greater reduction for the heavier M complexes. However, the fact that all the complexes exhibited the E_1 values lower by 0.2—0.3 V than the corresponding OEP–M suggests an existence of a through-space interaction between two constituent OEP–M rings, which results in pushing the HOMO level up so efficiently as to accelerate the electron-releasing even from the heavier metal complexes such as **8** and **22** which exist in

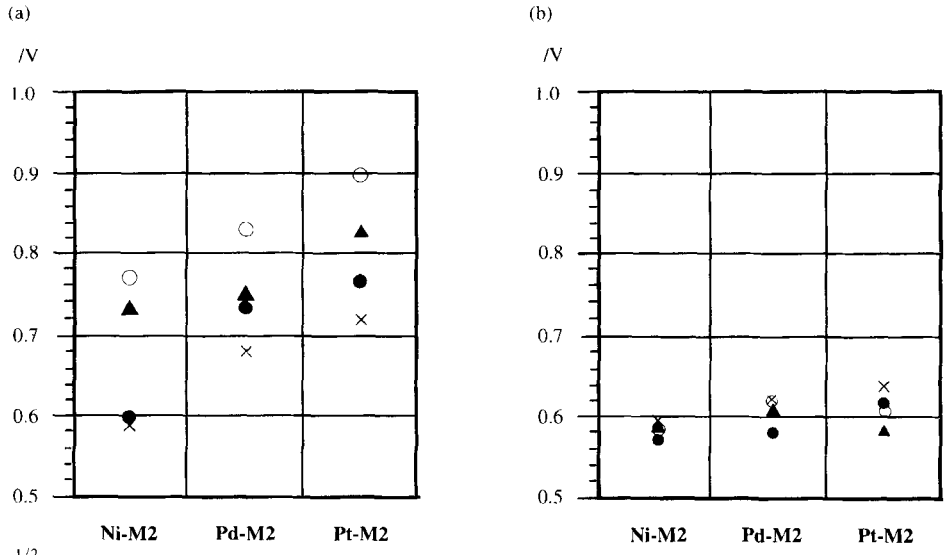

Fig. 7. Plots of $E_1^{1/2}$ values (a) for the (*E*)-bis(OEP)–(M1–M2) complexes and (b) for the corresponding (*Z*)-isomers. Each symbol in (a) and (b) indicates H_2 (×), Ni (●), Pd (▲), and Pt (○).

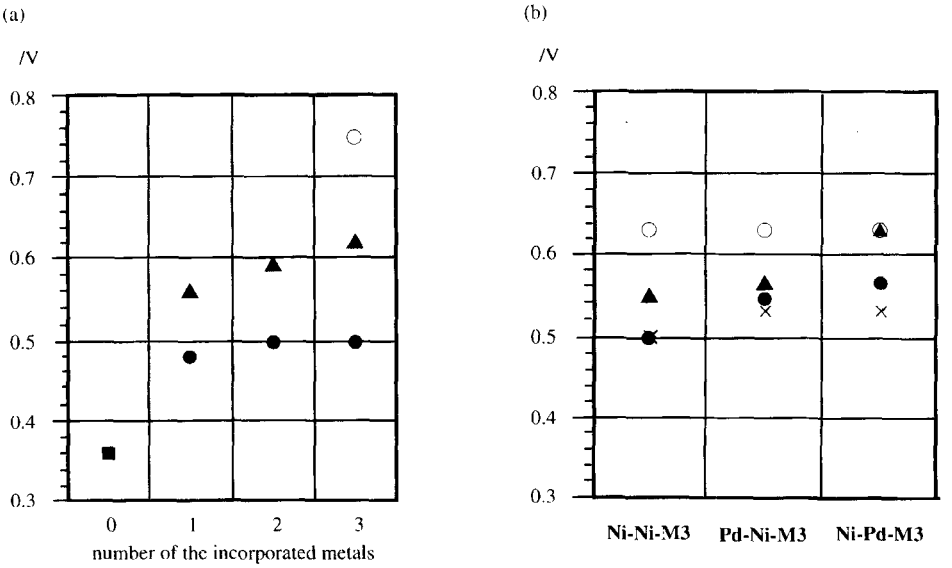

Fig. 8. Plots of $E_1^{1/2}$ values (a) for the uni-metallated complexes as against the number of the incorporated metals to FB **13** (symbol ■) and (b) for the mixed M1–M2–M3 complexes. Each symbol in (a) and (b) indicates H_2 (×), Ni (●), Pd (▲), and Pt (○).

the stairway-like conformations. The reversed order of the electron-releasing abilities in M = H_2 and M = Ni between bis(OEP)–M (**6** and **17**) and OEP–M (**1** and **2**) would also be attributable to such a through-space interaction, as a result.

On the other hand, the (*Z*)-isomeric series exhibited little changes of their E_1 values to be first oxidized at ca. 0.6 V, resulting in the fairly high electron-releasing abilities for all the complexes comparable to that for **17** (Fig. 7(b)). Particularly in the case of the heavy metal complexes such as **12** and **28**, the E_1 values are much lower than those of the corresponding (*E*)-isomers and OEP–M by ca. 0.3 and ca. 0.45 V, respectively. Although the transannular interaction between two faced OEP–M rings is not so intensive as to change their absorption spectra dramatically, it plays an important role in pushing the HOMO level up efficiently as well. Especially in the heavier metal complexes, such a transannular interaction is expected to be intensive enough to pull back these sterically repulsive OEP–M rings to interact with each other,[16] in agreement with the smaller dihedral angle between them (see Section III).

The more striking difference in their electron-releasing abilities can be seen in the respective pairs of the (*E*)- and (*Z*)-bis(OEP)–(M1–H_2) complexes. The (*E*)-(M1–H_2) complex exhibited the highest electron-releasing ability among each series of (*E*)-(M1–M2), while the (*Z*)-(M1–H_2) complex apparently exhibited the lowest electron-releasing ability among each series of (*Z*)-(M1–M2) in spite of a small degree scale. This result also indicates that the transannular interaction between the two metallated OEP–M1 and OEP–M2 rings is attractive to push up HOMO level more efficiently than the corresponding OEP–M1 and OEP–H_2 rings (also see Sections III and V).

(VIII) Tris(OEP)–(M1–M2–M3): The symmetrical tris(OEP)–M complexes were oxidized via three processes to afford the corresponding final products assignable to tris(dication)s,[6] while the unsymmetrical ones were oxidized mostly via four processes to the final products under the same conditions. It is interesting to mention that all the mixed complexes exhibited the two-electron transfer at the first stage, similarly to the uni-metallated tris(OEP)–M ones. As shown in Fig. 8(a), the electron-releasing abilities of the symmetrical and/or unsymmetrical uni-metallated tris(OEP)–M complexes increased further, as compared with those of the (*E*)-bis(OEP)–M complexes. However, these results also clearly show that the electron-releasing abilities decrease with increasing the number of the incorporated metals. Moreover, the decreasing magnitudes of their electron-releasing abilities are greater for the heavier metal complexes, in parallel with the decreasing magnitudes of the π-electronic interactions between the constituent OEP–M rings, resulting in the highest electron-releasing ability of FB **13** (E_1 = 0.36 V) and oppositely in the lowest ability of the Pt complex **16** (E_1 = 0.75 V) (see Section VI).

On the other hand, all the mixed complexes were proved to possess the medium electron-releasing abilities, as compared with the uni-metallated complexes, exhibiting smaller changes of the E_1 values in a potential region between 0.5 and 0.63 V (Fig. 8(b)). Nevertheless, the electron-releasing abilities are similarly observed as decreasing distinctly with an incorporation of the heavier metals. It is also proved that the Ni–Ni–M3 complexes are more susceptive to the heavy metal effect on the electron-releasing ability than the Ni–Pd–M3 complexes, though isomeric pairs of the Ni–Ni–Pd (**35**: E_1 = 0.55 V) and Ni–Pd–Ni (**37**: E_1 = 0.57 V) complexes exhibit almost the same electron-releasing abilities. The Ni–Pd–M3 complexes, however, exhibited substantially no difference of the electron-releasing ability from the isomeric Pd–Ni–M3 complexes, though only a pair of the Ni–Pd–Pd (**38**: E_1 = 0.63 V) and Pd–Ni–Pd (**40**: E_1 = 0.57 V) complexes was distinguishable. Although the reason why all the complexes of the Ni–Ni–Pt (**36**), Ni–Pd–Pt (**39**), and Pd–Ni–Pt (**41**) exhibited almost the same E_1 values of ca. 0.62 V should wait for further studies, it might be concluded that the electron-releasing abilities are more reduced for the complex carrying two consecutive heavier metal OEP rings.

Conclusion

Various vinylene-bridged bis(OEP)–(M1–M2) and tris(OEP)–(M1–M2–M3) complexes were conclusively synthesized by step-by-step and selective metallations of the respective FB **5**, **9**, and **13**. The structural properties were studied by means of ^{1}H NMR and electronic spectral measurements, proving that metallations with d^8 transition-metal ions stabilize the respective FB rings of **5** and **13** due to the back-donation interactions and hence induce the metallated OEP rings to twist about the vinylene linkage. This brings the π-electronic conjugation planarity through the vinylene linkage to destruction to afford the stairway-like conformation, where the magnitude of deformation of each OEP–M ring from the molecular plane throughout the vinylene linkage is greater for the heavier metal OEP ring. The electron-releasing abilities were studied by means of cyclic voltammetry and were estimated from the first half-wave oxidation E_1 values. Tris(OEP)–H_2–H_2–H_2 (**13**) reduced its electron-releasing ability regularly on metallations and more intensively for the heavier metal complexes. Although the pair of isomers (ex. **38** and **40**) did not exhibit a large difference in the electron-releasing abilities of tris(OEP)–(M1–M2–M3), the results indicate that the complex (**38**) carrying two consecutive heavier metal OEP rings possesses the lower ability than another (**40**). On the other hand, the (*E*)-bis(OEP)–(M1–M2) complexes exhibited a similar trend to the tris(OEP)–(M1–M2–M3) complexes, while the (*Z*)-bis(OEP)–(M1–M2) complexes showed little dependence of the electron-releasing abilities upon the incorporated metals M.

As a next stage, some studies on their properties caused by selective activation of the particular OEP–M ring in the tris(OEP)–(M1–M2–M3) complexes are now in progress.

Experimental

The melting points were determined on a hot-stage apparatus and are uncorrected. IR spectra were measured on a JASCO FT/IR 7300 spectrophotometer as KBr disks; only significant absorptions are reported. Electronic absorption spectra were measured in $CHCl_3$ solution on a Shimadzu UV-2200A spectrophotometer; shoulder and weak absorption bands are abbreviated as sh and WAB, respectively. ^{1}H NMR spectra were measured in $CDCl_3$ solution on a JEOL α-400 (400 MHz) spectrometer and were recorded in δ-values with TMS as an internal standard. The coupling constants (*J*) are given in Hz. FAB mass spectra were recorded with a JEOL AX-505 spectrometer using m-nitrobenzyl alcohol (NBA) as a matrix agent. Cyclic voltammetry was performed on a BAS CV-27 potentiometer in CH_2Cl_2 containing *n*-Bu_4NClO_4, under the electrochemical conditions of GC (working E), Pt (counter E), and SCE (reference E) at the scan rate of 120 mV s^{-1}.[6] Silica gel (Fuji Silysia gel BW 820MH or BW 127ZH) was used for column chromatography. $CHCl_3$ was distilled over calcium hydride before use. The reactions were followed by TLC aluminum sheets precoated with Merck silica gel F_{254} or with Merck aluminum oxide GF_{254}. Organic extracts were dried over anhydrous sodium sulfate or magnesium sulfate prior to removal of the solvents. The OEP–M complexes **2**,[7a] **3**,[7b] and **4**[7b] and the FB **5**,[3] **9**,[8] and **13**[2] as the starting materials for the title mixed complexes were prepared according to the reported procedures.

Nickel(II)–FB Complex of (*E*)-5,5′-Vinylenebis(2,3,7,8,12,13,17,18-octaethylporphyrin) (17): A solution of **5** (52 mg, 0.048 mmol) in $CHCl_3$ (30 cm^3) was gently refluxed for 30 min. Into this solution, $Ni(OAc)_2 \cdot 4H_2O$ (11.9 mg, 0.048 mmol) in MeOH (6 cm^3) was added. The mixture was refluxed for 1 h. After being poured into water, the reaction mixture was extracted with $CHCl_3$, washed with brine, and then dried. The residue obtained after removal of solvent was chromatographed on silica gel (4.2×18 cm) with $CHCl_3$ to afford the Ni–Ni complex **6**[6,8] (3.5 mg, 12% based on $Ni(OAc)_2 \cdot 4H_2O$) from the first fractions. From the later fractions with $CHCl_3$–AcOEt (19 : 1) were obtained the Ni–H_2 complex **17** (17.6 mg, 32%) and the starting material **5** (16 mg, 31%) successively.

17: Black purple microcrystals (hexane–$CHCl_3$); Mp, gradual decomposition above 230 °C; Mass (FAB) *m/z* 1151 (M^++1); IR (KBr) 3295 (NH), 2965, 2930, and 2870 cm^{-1} (CH); ^{1}H NMR

δ = 10.08 (2H, s, *meso*-H), 9.91 (1H, s, *meso*-H), 9.55 (2H, s, *meso*-H), 9.54 (1H, s, *meso*-H), 8.19 (1H, d, J = 16 Hz, –CH=CH–), 8.07 (1H, d, J = 16 Hz, –CH=CH–), 4.1—3.5 (32H, m, $-CH_2-$), 2.0—0.9 (48H, m, CH_3), and −2.83 (2H, br s, NH); Vis-uv λ_{max} 297 (sh 19000), 329 (sh 25000), 405 (sh 170000), 418 (206000), 508 (sh 27500), 537 (sh 19500), 574 (18500), 632 (6000), and WAB up to 900 nm. Found: C, 77.01; H, 8.03; N, 9.55%. Calcd for $C_{74}H_{90}N_8Ni$: C, 77.27; H, 7.89; N, 9.74%.

Palladium(II)–FB Complex of (*E*)-5,5′-Vinylenebis(2,3,7,8,12,13,17,18-octaethylporphyrin) (18): A solution of **5** (30 mg, 0.027 mmol) in $CHCl_3$ (25 cm^3) was gently refluxed for 30 min. Into this solution, $Pd(OAc)_2$ (6.1 mg, 0.027 mmol) in MeOH (5 cm^3) was added. The mixture was refluxed for 1 h. After being poured into water, the reaction mixture was extracted with $CHCl_3$, washed with brine, and then dried. The residue obtained after removal of solvent was chromatographed on silica gel (3.2×19 cm) with $CHCl_3$ to afford the Pd–Pd complex **7**[6] (3.5 mg, 20% based on $Pd(OAc)_2$) from the first fractions. The later fractions with $CHCl_3$–AcOEt (19 : 1) afforded the Pd–H_2 complex **18** (12 mg, 37%) and the starting material **5** (9.5 mg, 32%) successively.

18: Deep purple microcrystals (hexane–$CHCl_3$); Mp, gradual decomposition above 250 °C; Mass (FAB) *m/z* 1199 (M^++1); IR (KBr) 3300 (NH), 2965, 2930, and 2870 cm^{-1} (CH); ^{1}H NMR δ = 10.14 (2H, s, *meso*-H), 10.11 (2H, s, *meso*-H), 10.03 (1H, s, *meso*-H), 9.96 (1H, s, *meso*-H), 8.48 (2H, d, J = 16 Hz, –CH=CH–), 8.23 (2H, d, J = 16 Hz, –CH=CH–), 4.1—3.5 (32H, m, $-CH_2-$), 2.0—0.8 (48H, m, CH_3), and −2.87 (2H, br s, NH); Vis-uv λ_{max} 278 (16700), 324 (sh 21000), 402 (sh 177000), 419 (230000), 518 (22500), 533 (22300), 564 (sh 17800), 590 (sh 6300), 633 (3300), and WAB up to 850 nm. Found: C, 74.11; H, 7.87; N, 9.11%. Calcd for $C_{74}H_{90}N_8Pd$: C, 74.19; H, 7.57; N, 9.35%.

Platinum(II)–FB Complex of (*E*)-5,5′-Vinylenebis(2,3,7,8,12,13,17,18-octaethylporphyrin) (19): (a) $PtCl_2$ (12.2 mg, 0.046 mmol) in AcOH (3 cm^3) was heated at 60 °C for 1 h. Into this solution was added a solution of **5** (10 mg, 0.0091 mmol) in $CHCl_3$ (10 cm^3). The mixture was refluxed for 17 h. After being poured into water and neutralized with sat. $NaHCO_3$ aq, the reaction mixture was extracted with $CHCl_3$, washed with brine, and then dried. The residue obtained after removal of solvent was chromatographed on silica gel (3.2×15 cm) with $CHCl_3$ to afford a trace of the Pt–Pt complex **8**.[6] Further fractions with $CHCl_3$–AcOEt (19 : 1) afforded the Pt–H_2 complex **19** (1.2 mg, 10%) and the starting material **5** (4 mg, 40%) successively. From the final fractions with $CHCl_3$–AcOEt (5 : 1) was obtained a very little amount of (*Z*)-isomeric FB **9**.

(b) [Pt(acac)$_2$] (14.2 mg, 0.036 mmol) in AcOH (6 cm^3) was gently refluxed for 30 min. Into this solution, a solution of **5** (10 mg, 0.0091 mmol) in AcOH (8 cm^3) was added. The mixture was refluxed for 4.5 h. After being poured into water and neutralized with sat. $NaHCO_3$ aq, the reaction mixture was extracted with $CHCl_3$, washed with brine, and then dried. Procedures for separation of the mixture similar to those in the reaction (a) afforded **8** (1 mg, 7.4%), **19** (2.2 mg, 19%), and **5** (1.9 mg, 19%). The (*Z*)-isomeric Pt–H_2 complex **25** (2 mg, 17%, see below) and the (*Z*)-isomeric FB **9** (1 mg, 10%) were also successively obtained from the further fractions by column chromatography.

19: Deep purple microcrystals (hexane–$CHCl_3$); Mp, gradual decomposition above 250 °C; Mass (FAB) *m/z* 1287 (M^++1); IR (KBr) 3300 (NH), 2965, 2930, and 2870 cm^{-1} (CH); ^{1}H NMR δ = 10.14 (2H, s, *meso*-H), 10.03 (2H, s, *meso*-H), 9.97 (1H, s, *meso*-H), 9.96 (1H, s, *meso*-H), 8.43 (2H, d, J = 16 Hz, –CH=CH–), 8.29 (2H, d, J = 16 Hz, –CH=CH–), 4.0—3.4 (32H, m, $-CH_2-$), 2.1—0.8 (48H, m, CH_3), and −2.89 (2H, br s, NH); Vis-uv λ_{max} 393 (207000), 415 (247000), 513 (28600), 543 (35000), 578 (7900), 633 (2800), and WAB up to 800 nm. Found: C, 68.88; H, 7.37; N, 8.55%. Calcd for $C_{74}H_{90}N_8Pt$: C, 69.08; H, 7.05; N, 8.71%.

Nickel(II)–Palladium(II) Complex of (*E*)-5,5′-Vinylenebis(2,3,7,8,12,13,17,18-octaethylporphyrin) (20): A solution of **17** (5.5 mg, 0.0048 mmol) in $CHCl_3$ (5 cm^3) was admixed with a solution of $Pd(OAc)_2$ (5.4 mg, 0.024 mmol) in MeOH (1.2 cm^3). The mixture was stirred at room temperature for 1.5 h. After being poured into water, the reaction mixture was extracted with $CHCl_3$, washed with brine, and then dried. The residue obtained after removal of solvent was chromatographed on silica gel (2.6×10 cm) with $CHCl_3$ to afford the Ni–Pd complex **20** (5.4 mg, 90%).

20: Black purple microcrystals (hexane–$CHCl_3$); Mp > 300 °C; Mass (FAB) *m/z* 1255 (M^++1); IR (KBr) 2960, 2930, and 2870 cm^{-1} (CH); ^{1}H NMR δ = 10.07 (2H, s, *meso*-H), 10.01 (1H, s, *meso*-H), 9.58 (1H, s, *meso*-H), 9.57 (2H, s, *meso*-H), 8.02 (1H, d, J = 15 Hz, –CH=CH–), 7.90 (1H, d, J = 15 Hz, –CH=CH–), 4.1—3.5 (32H, m, $-CH_2-$), and 2.0—0.8 (48H, m, CH_3); Vis-uv λ_{max} 336 (sh 16300), 402 (sh 118000), 416 (153000), 527 (16100), 553 (sh 19800), 561 (22000), and WAB up to 700 nm. Found: C, 70.55; H, 7.32; N, 8.66%. Calcd for $C_{74}H_{88}N_8NiPd$: C, 70.84; H, 7.07; N, 8.93%.

Nickel(II)–Platinum(II) Complex of (*E*)-5,5′-Vinylenebis(2,3,7,8,12,13,17,18-octaethylporphyrin) (21): A solution of $PtCl_2$ (31.9 mg, 0.12 mmol) in AcOH (5 cm^3) was refluxed for 2 h. Into this solution was added a solution of **17** (18.8 mg, 0.016 mmol) in $CHCl_3$ (15 cm^3) at 60 °C in portions. The mixture was refluxed for 20 h. After being poured into water and neutralized with sat. $NaHCO_3$ aq, the reaction mixture was extracted with $CHCl_3$, washed with brine, and then dried. The residue obtained after removal of solvent was chromatographed on silica gel (3.2×12 cm) with $CHCl_3$ to afford the Ni–Pt complex **21** (7.3 mg, 33%) and with $CHCl_3$–AcOEt (19 : 1) to recover the starting material **17** (6.5 mg, 35%) successively.

21: Deep purple microcrystals (hexane–$CHCl_3$); Mp > 300 °C; Mass (FAB) *m/z* 1344 (M^++1); IR (KBr) 2965, 2930, and 2870 cm^{-1} (CH); ^{1}H NMR δ = 9.99 (2H, s, *meso*-H), 9.94 (1H, s, *meso*-H), 9.58 (1H, s, *meso*-H), 9.57 (2H, s, *meso*-H), 7.97 (2H, br s, –CH=CH–), 4.1—3.5 (32H, m, $-CH_2-$), and 2.0—0.8 (48H, m, CH_3); Vis-uv λ_{max} 298 (9800), 392 (161000), 411 (187000), 515 (11200), 543 (23300), 551 (sh 19700), 572 (sh 11900), and WAB up to 700 nm. Found: C, 65.95; H, 6.63; N, 8.09%. Calcd for $C_{74}H_{88}N_8NiPt$: C, 66.16; H, 6.60; N, 8.34%.

Palladium(II)–Platinum(II) Complex of (*E*)-5,5′-Vinylenebis-(2,3,7,8,12,13,17,18-octaethylporphyrin) (22): A solution of $PtCl_2$ (6.0 mg, 0.023 mmol) in PhCN (2 cm^3) was gently refluxed for 30 min. Into this solution, **18** (13.5 mg, 0.011 mmol) as solid was added. The mixture was refluxed for 2 h. After being poured into water, the reaction mixture was extracted with $CHCl_3$. The extracts were washed with brine and were dried. The residue obtained after removal of solvent was chromatographed on silica gel (3.2×15 cm) with hexane–$CHCl_3$ (1 : 1) to afford the Pd–Pt complex **22** (5.0 mg, 32%) and a trace of the (*Z*)-isomeric Pd–Pt complex **28** (see below), together with the insoluble materials.

22: Reddish purple microcrystals (hexane–$CHCl_3$); Mp > 300 °C; Mass (FAB) *m/z* 1392 (M^++1); IR (KBr) 2960, 2925, and 2850 cm^{-1} (CH); ^{1}H NMR δ = 10.10 (2H, s, *meso*-H), 10.03 (1H, s, *meso*-H), 10.02 (2H, s, *meso*-H), 9.96 (1H, s, *meso*-H), 8.23 (1H, d, J = 15 Hz, –CH=CH–), 8.10 (1H, d, J = 15 Hz, –CH=CH–), 4.2—3.4 (32H, m, $-CH_2-$), and 2.0—0.8 (48H, m, CH_3); Vis-uv λ_{max} 277 (21400), 290 (sh 20700), 332 (20400), 393 (195000), 411 (254000), 522 (24900), 542 (sh 34800), 553 (44800), and 565 nm (sh 18900).

Found: C, 63.55; H, 6.61; N, 7.84%. Calcd for $C_{74}H_{88}N_8PdPt$: C, 63.89; H, 6.38; N, 8.06%.

Nickel(II)–FB Complex of (*Z*)-5,5′-Vinylenebis(2,3,7,8,12,13,17,18-octaethylporphyrin) (23): A solution of **9** (15 mg, 0.014 mmol) in $CHCl_3$ (15 cm^3) was gently refluxed for 30 min. Into this solution, $Ni(OAc)_2 \cdot 4H_2O$ (3.5 mg, 0.014 mmol) in MeOH (3 cm^3) was added. The mixture was refluxed for 7 h. After being poured into water, the reaction mixture was extracted with $CHCl_3$, washed with brine, and then dried. The residue obtained after removal of solvent was chromatographed on silica gel (3.2×7 cm) with $CHCl_3$–AcOEt (4 : 1) to afford a very little amount of the (*E*)- and (*Z*)-isomeric Ni–Ni complexes (**6**[6,8] and/or **10**[6,8]) which were deduced on the basis of absorption and MS spectral results. The later fractions afforded the (*E*)-isomeric Ni–H_2 complex **17** (1.0 mg, 6.3%), the desired (*Z*)-isomeric Ni–H_2 complex **23** (7.1 mg, 45%), and the starting material **9** (2.1 mg, 14%) successively.

23: Black purple microcrystals ($CHCl_3$–MeOH); Mp, gradual decomposition above 250 °C; Mass (FAB) *m/z* 1151 (M^++1); IR (KBr) 3295 (NH), 2960, 2930, and 2870 cm^{-1} (CH); ^{1}H NMR δ = 9.66 (1H, s, *meso*-H), 9.49 (1H, d, *J* = 11 Hz, –CH=CH–), 9.32 (1H, d, *J* = 11 Hz, –CH=CH–), 9.00 (1H, s, *meso*-H), 8.49 (2H, s, *meso*-H), 7.76 (2H, s, *meso*-H), 4.5—2.5 (32H, m, $-CH_2-$), 2.0—0.6 (48H, m, CH_3), and −4.75 and −5.64 (1H each, br s, NH); Vis-uv λ_{max} 305 (sh 28000), 393 (187000), 524 (14000), 555 (sh 11200), 588 (11000), and 645 nm (3200). Found: C, 76.98; H, 8.22; N, 9.50%. Calcd for $C_{74}H_{90}N_8Ni$: C, 77.27; H, 7.89; N, 9.74%.

Palladium(II)–FB Complex of (*Z*)-5,5′-Vinylenebis(2,3,7,8,12,13,17,18-octaethylporphyrin) (24): A solution of **9** (15 mg, 0.014 mmol) in $CHCl_3$ (15 cm^3) was gently refluxed for 30 min. Into this solution, $Pd(OAc)_2$ (3.1 mg, 0.014 mmol) in MeOH (3 cm^3) was added. The mixture was refluxed for 1 h. After being poured into water, the reaction mixture was extracted with $CHCl_3$, washed with brine, and then dried. The residue obtained after removal of solvent was chromatographed on silica gel (3.2×8 cm) with $CHCl_3$–AcOEt (4 : 1) to afford traces of the (*E*)- and (*Z*)-isomeric Pd–Pd complexes (**7**[6] and/or **11**[6]) which were deduced on the basis of absorption and MS spectral results. The later fractions afforded the (*E*)-isomeric Pd–H_2 complex **18** (1.2 mg, 7.3%), the desired (*Z*)-isomeric Pd–H_2 complex **24** (6.4 mg, 39%), and the starting material **9** (5.4 mg, 36%) successively.

24: Reddish purple microcrystals ($CHCl_3$–MeOH); Mp, gradual decomposition above 250 °C; Mass (FAB) *m/z* 1199 (M^++1); IR (KBr) 3295 (NH), 2960, 2930, and 2870 cm^{-1} (CH); ^{1}H NMR δ = 9.70 (1H, d, *J* = 11 Hz, –CH=CH–), 9.54 (1H, d, *J* = 11 Hz, –CH=CH–), 9.46 (1H, s, *meso*-H), 9.35 (1H, s, *meso*-H), 8.08 (2H, s, *meso*-H), 8.07 (2H, s, *meso*-H), 4.5—2.6 (32H, m, $-CH_2-$), 2.1—0.8 (48H, m, CH_3), and −5.68 and −6.47 (1H each, br s, NH); Vis-uv λ_{max} 325 (sh 35800), 391 (190000), 529 (13500), 563 (sh 11400), 574 (sh 11200), and 648 nm (2900). Found: C, 73.81; H, 7.78; N, 9.33%. Calcd for $C_{74}H_{90}N_8Pd$: C, 74.19; H, 7.57; N, 9.35%.

Platinum(II)–FB Complex of (*Z*)-5,5′-Vinylenebis(2,3,7,8,12,13,17,18-octaethylporphyrin) (25): A solution of **9** (10 mg, 0.0091 mmol) in AcOH (10 cm^3) was refluxed for 30 min. Into this solution, a solution of [Pt(acac)$_2$] (14.2 mg, 0.036 mmol) in AcOH (4 cm^3) was added. The mixture was refluxed for 4.5 h. After being poured into water and neutralized with sat. $NaHCO_3$ aq, the reaction mixture was extracted with $CHCl_3$, washed with brine, and then dried. The residue obtained after removal of solvent was chromatographed on silica gel (3.2×8 cm) with $CHCl_3$ to afford a trace of the (*E*)- and (*Z*)-isomeric Pt–Pt complexes (**8**[6] and/or **12**[6]) which were deduced on the basis of absorption and MS spectral results. The later fractions with $CHCl_3$–AcOEt (4 : 1) afforded the (*E*)-isomeric Pt–H_2 complex **19** (1.2 mg, 10%) and the desired (*Z*)-isomeric Pt–H_2 complex **25** (2.1 mg, 18%) successively. The starting material **9** (3.6 mg, 36%) was recovered from the final fractions.

25: Reddish purple microcrystals ($CHCl_3$–MeOH); Mp, gradual decomposition above 250 °C; Mass (FAB) *m/z* 1287 (M^++1); IR (KBr) 3300 (NH), 2965, 2930, and 2870 cm^{-1} (CH); ^{1}H NMR δ = 9.62 (1H, d, *J* = 11 Hz, –CH=CH–), 9.54 (1H, d, *J* = 11 Hz, –CH=CH–), 9.47 (1H, s, *meso*-H), 9.26 (1H, s, *meso*-H), 8.10 (2H, s, *meso*-H), 7.96 (2H, s, *meso*-H), 4.5—2.5 (32H, m, $-CH_2-$), 2.0—0.8 (48H, m, CH_3), and −5.62 and −6.48 (1H each, br s, NH); Vis-uv λ_{max} 325 (35800), 383 (180000), 524 (13000), 555 (12500), 563 (sh 11400), 574 (sh 11200), and 648 nm (2800). Found: C, 69.00; H, 7.18; N, 8.65%. Calcd for $C_{74}H_{90}N_8Pt$: C, 69.08; H, 7.05; N, 8.71%.

Nickel(II)–Palladium(II) Complex of (*Z*)-5,5′-Vinylenebis(2,3,7,8,12,13,17,18-octaethylporphyrin) (26): The mixture of **23** (6.0 mg, 0.0052 mmol) and $Pd(OAc)_2$ (5.0 mg, 0.022 mmol) in a 5 : 1 mixture of $CHCl_3$ with MeOH (10 cm^3) was stirred at room temperature for 2.5 h. After being poured into water, the reaction mixture was extracted with $CHCl_3$, washed with brine, and then dried. The residue obtained after removal of solvent was chromatographed on silica gel (3.2×8 cm) with hexane–$CHCl_3$ (3 : 2) to afford the (*E*)-isomeric Ni–Pd complex **20** (0.8 mg, 12%) and the desired (*Z*)-isomeric Ni–Pd complex **26** (5.6 mg, 86%) successively.

26: Black purple microcrystals ($CHCl_3$–MeOH); Mp > 300 °C; Mass (FAB) *m/z* 1255 (M^++1); IR (KBr) 2965, 2930, and 2870 cm^{-1} (CH); ^{1}H NMR δ = 9.67 (1H, s, *meso*-H), 9.43 (1H, d, *J* = 11 Hz, –CH=CH–), 9.32 (1H, d, *J* = 11 Hz, –CH=CH–), 8.81 (1H, s, *meso*-H), 8.44 (2H, s, *meso*-H), 7.80 (2H, s, *meso*-H), 4.4—2.8 (32H, m, $-CH_2-$), and 2.0—0.8 (48H, m, CH_3); Vis-uv λ_{max} 290 (16000), 335 (sh 21000), 392 (186000), 537 (sh 11800), and 567 nm (15300). Found: C, 70.61; H, 7.28; N, 8.66%. Calcd for $C_{74}H_{88}N_8NiPd$: C, 70.84; H, 7.07; N, 8.93%.

Nickel(II)–Platinum(II) Complex of (*Z*)-5,5′-Vinylenebis(2,3,7,8,12,13,17,18-octaethylporphyrin) (27): (a) The mixture of **23** (5.0 mg, 0.0043 mmol) and $Pt(acac)_2$ (15.7 mg, 0.040 mmol) in PhOH (5 cm^3) was stirred at 150 °C for 4.5 h. After being poured into water, the reaction mixture was extracted with $CHCl_3$, washed with brine, and then dried. The residue obtained after removal of solvent was chromatographed on silica gel (3.2×8 cm) with $CHCl_3$ to afford only traces of the (*E*)- and (*Z*)-isomeric Ni–Pt complexes, which were deduced on the basis of absorption and MS spectral results, together with some insoluble materials.

(b) The mixture of **25** (5.0 mg, 0.0039 mmol) and $Ni(OAc)_2 \cdot 4H_2O$ (49.7 mg, 0.20 mmol) in a mixture of $CHCl_3$ and MeOH (16 cm^3, 5 : 3) was refluxed for 15 h. After being poured into water, the reaction mixture was extracted with $CHCl_3$, washed with brine, and then dried. The residue obtained after removal of solvent was chromatographed on silica gel (3.2×5 cm) with $CHCl_3$ to afford the desired Ni–Pt complex **27** (5.2 mg, 100%).

27: Reddish purple microcrystals ($CHCl_3$–MeOH); Mp > 300 °C; Mass (FAB) *m/z* 1344 (M^++1); IR (KBr) 2960, 2930, and 2870 cm^{-1} (CH); ^{1}H NMR δ = 9.57 (1H, s, *meso*-H), 9.41 (1H, d, *J* = 11 Hz, –CH=CH–), 9.25 (1H, d, *J* = 11 Hz, –CH=CH–), 8.82 (1H, s, *meso*-H), 8.34 (2H, s, *meso*-H), 7.82 (2H, s, *meso*-H), 4.4—2.8 (32H, m, $-CH_2-$), and 2.0—0.6 (48H, m, CH_3); Vis-uv λ_{max} 304 (25500), 385 (175000), 520 (sh 11200), 555 (17000), and 588 nm (sh 8200). Found: C, 65.78; H, 6.54; N, 8.09%. Calcd for $C_{74}H_{88}N_8NiPt$: C, 66.16; H, 6.60; N, 8.34%.

Palladium(II)–Platinum(II) Complex of (*Z*)-5,5′-Vinylenebis-(2,3,7,8,12,13,17,18-octaethylporphyrin) (28): (a) The mixture of **24** (5.0 mg, 0.0042 mmol) and $Pt(acac)_2$ (16.2 mg, 0.041 mmol) in PhOH (5 cm^3) was stirred at 150 °C for 4.5 h. After being poured into water, the reaction mixture was extracted with $CHCl_3$, washed with brine, and then dried. The residue obtained after removal of solvent was chromatographed on silica gel (3.2×6 cm) with hexane–$CHCl_3$ (9 : 1) to afford only traces of the (*E*)- and (*Z*)-isomeric Pd–Pt complexes which were deduced on the basis of absorption and MS spectral results.

(b) The mixture of **25** (5.0 mg, 0.0039 mmol) and $Pd(OAc)_2$ (8.7 mg, 0.039 mmol) in a mixture of $CHCl_3$ and MeOH (7 cm^3, 5 : 2) was stirred at room temperature for 1 h. After being poured into water, the reaction mixture was extracted with $CHCl_3$, washed with brine, and then dried. Similarly, separation of the products by column chromatography on silica gel afforded the (*E*)-isomeric Pd–Pt complex **22** (0.6 mg, 11%) from the first fractions and the desired (*Z*)-isomeric Pd–Pt complex **28** (4.6 mg, 85%) from the second fractions successively.

28: Sparklingly reddish purple microcrystals ($CHCl_3$–MeOH); Mp > 300 °C; Mass (FAB) *m/z* 1392 (M^++1); IR (KBr) 2960, 2930, and 2870 cm^{-1} (CH); ^1H NMR δ = 9.54 (1H, d, *J* = 11 Hz, –CH=CH–), 9.46 (1H, d, *J* = 11 Hz, –CH=CH–), 9.27 (1H, s, *meso*-H), 9.16 (1H, s, *meso*-H), 8.18 (2H, s, *meso*-H), 8.05 (2H, s, *meso*-H), 4.5—3.0 (32H, m, $-CH_2-$), and 2.0—1.0 (48H, m, CH_3); Vis-uv λ_{max} 290 (24000), 384 (200000), 531 (sh 13700), 548 (sh 16000), 560 (18400), and 578 nm (sh 12000). Found: C, 63.66; H, 6.51; N, 7.77%. Calcd for $C_{74}H_{88}N_8PdPt$: C, 63.89; H, 6.38; N, 8.06%.

FB–Nickel(II)–FB and Nickel(II)–Nickel(II)–FB Complexes of (*E*,*E*)-5,15-Bis[2-(2,3,7,8,12,13,17,18-octaethyl-5-porphyrinyl)vinyl]-2,3,7,8,12,13,17,18-octaethylporphyrin (29 and 30): A solution of **13** (23 mg, 0.014 mmol) in $CHCl_3$ (10 cm^3) was admixed with a solution of $Ni(OAc)_2{\cdot}4H_2O$ (3.3 mg, 0.013 mmol) in MeOH (2 cm^3). The mixture was stirred with gentle reflux for 1 h. After being poured into water, the reaction mixture was extracted with $CHCl_3$, washed with brine, and then dried. The residue obtained after removal of solvent was chromatographed on silica gel (3.4×15 cm) with $CHCl_3$ to afford a trace of the Ni–Ni–Ni complex **14**[2,6] from the first fractions. Further fractions with $CHCl_3$–AcOEt (30 : 1) afforded the Ni–Ni–H_2 complex **30** (3 mg, 24% based on $Ni(OAc)_2{\cdot}4H_2O$) and the H_2–Ni–H_2 complex **29** (7.7 mg, 32% based on $Ni(OAc)_2{\cdot}4H_2O$) successively. The starting material **13** (7 mg, 30%) was recovered from the final fractions with $CHCl_3$–AcOEt (1 : 1).

29: Black purple microcrystals (hexane–$CHCl_3$); Mp > 300 °C; Mass (FAB) *m/z* 1710 (M^++1); IR (KBr) 3300 (NH), 2960, 2930, and 2870 cm^{-1} (CH); ^1H NMR δ = 10.05 (4H, s, *meso*-H), 9.91 (2H, s, *meso*-H), 9.42 (2H, s, *meso*-H), 8.12 (2H, d, *J* = 15 Hz, –CH=CH–), 8.08 (2H, br d, *J* = 15 Hz, –CH=CH–), 4.2—3.4 (48H, m, CH_2), 2.0—0.8 (72H, m, CH_3), and −2.81 (4H, br s, NH); Vis-uv λ_{max} 322 (sh 33000), 378 (sh 118000), 414 (267000), 507 (55500), 543 (29500), 580 (28000), 632 (sh 10000), and WAB up to 1000 nm. Found: C, 78.65; H, 8.19; N, 9.62%. Calcd for $C_{112}H_{136}N_{12}Ni$: C, 78.71; H, 8.02; N, 9.83%.

30: Black purple microcrystals (hexane–$CHCl_3$); Mp > 300 °C; Mass (FAB) *m/z* 1766 (M^++1); IR (KBr) 3300 (NH), 2960, 2930, and 2870 cm^{-1} (CH); ^1H NMR δ = 10.03 (2H, s, *meso*-H), 9.90 (1H, s, *meso*-H), 9.51 (1H, s, *meso*-H), 9.46 (2H, s, *meso*-H), 9.37 (1H, s, *meso*-H), 9.34 (1H, s, *meso*-H), 8.05 (2H, s, –CH=CH–), 7.67 (1H, d, *J* = 15 Hz, –CH=CH–), 7.58 (1H, d, *J* = 15 Hz, –CH=CH–), 4.2—3.0 (48H, m, CH_2), 2.0—0.8 (72H, m, CH_3), and −2.80 (2H, br s, NH); Vis-uv λ_{max} 307 (sh 32000), 411 (256000), 424 (sh 212000), 505 (57000), 545 (sh 35000), 574 (31000), 630 (12500), and WAB up to 1000 nm. Found: C, 75.83; H, 7.77; N, 9.34%. Calcd for $C_{112}H_{134}N_{12}Ni_2$: C, 76.18; H, 7.65; N, 9.52%.

FB–Palladium(II)–FB and Palladium(II)–Palladium(II)–FB Complexes of (*E*,*E*)-5,15-Bis[2-(2,3,7,8,12,13,17,18-octaethyl-5-porphyrinyl)vinyl]-2,3,7,8,12,13,17,18-octaethylporphyrin (31 and 32): A solution of **13** (20 mg, 0.012 mmol) in $CHCl_3$ (10 cm^3) was admixed with a solution of $Pd(OAc)_2$ (2.7 mg, 0.012 mmol) in MeOH (2 cm^3). The mixture was stirred with gentle reflux for 5 h. After being poured into water, the reaction mixture was extracted with $CHCl_3$, washed with brine, and then dried. The residue obtained after removal of solvent was chromatographed on silica gel (3.4×15 cm) with $CHCl_3$ to afford the Pd–Pd–Pd complex **15**[6,11] (1.5 mg, 19% based on $Pd(OAc)_2$) from the first fractions. The fractions with $CHCl_3$–AcOEt (20 : 1) afforded the Pd–Pd–H_2 complex **32** (4.4 mg, 39% based on $Pd(OAc)_2$) and the H_2–Pd–H_2 complex **31** (4.7 mg, 22% based on $Pd(OAc)_2$) successively. The starting material **13** (2 mg, 10%) was recovered from the final fractions.

31: Deep purple microcrystals (hexane–$CHCl_3$); Mp > 300 °C; Mass (FAB) *m/z* 1757 (M^++1); IR (KBr) 3300 (NH), 2960, 2930, and 2870 cm^{-1} (CH); ^1H NMR δ = 10.12 (4H, s, *meso*-H), 9.99 (2H, s, *meso*-H), 9.98 (2H, s, *meso*-H), 8.48 (2H, d, *J* = 15 Hz, –CH=CH–), 8.12 (2H, br d, *J* = 15 Hz, –CH=CH–), 4.3—3.3 (48H, m, CH_2), 2.1—1.1 (72H, m, CH_3), and −2.88 (4H, br s, NH); Vis-uv λ_{max} 330 (sh 34000), 375 (sh 95000), 416 (271000), 426 (sh 255000), 509 (34500), 541 (28000), 557 (24600), 633 (7600), and WAB up to 800 nm. Found: C, 76.55; H, 8.02; N, 9.37%. Calcd for $C_{112}H_{136}N_{12}Pd$: C, 76.57; H, 7.80; N, 9.57%.

32: Purple microcrystals (hexane–$CHCl_3$); Mp > 300 °C; Mass (FAB) *m/z* 1862 (M^++1); IR (KBr) 3310 (NH), 2960, 2930, and 2870 cm^{-1} (CH); ^1H NMR δ = 10.12 (2H, s, *meso*-H), 10.09 (2H, s, *meso*-H), 10.05 (1H, s, *meso*-H), 9.99 (1H, s, *meso*-H), 9.98 (2H, s, *meso*-H), 8.47 (1H, d, *J* = 15 Hz, –CH=CH–), 8.16 (1H, d, *J* = 15 Hz, –CH=CH–), 8.10 (1H, br d, *J* = 15 Hz, –CH=CH–), 8.05 (1H, br d, *J* = 15 Hz, –CH=CH–), 4.3—3.4 (48H, m, CH_2), 2.2—1.8 (48H, m, CH_3), 1.4—1.1 (24H, m, CH_3), and −2.93 (2H, br s, NH); Vis-uv λ_{max} 330 (sh 34000), 412 (288000), 427 (sh 258000), 517 (sh 27500), 540 (29500), 553 (32500), 562 (sh 29500), 578 (sh 21000), 633 (4250), and WAB up to 700 nm. Found: C, 71.94; H, 7.57; N, 8.88%. Calcd for $C_{112}H_{134}N_{12}Pd_2$: C, 72.28; H, 7.26; N, 9.03%.

Nickel(II)–Palladium(II)–FB Complex of (*E*,*E*)-5,15-Bis[2-(2,3,7,8,12,13,17,18-octaethyl-5-porphyrinyl)vinyl]-2,3,7,8,12,13,17,18-octaethylporphyrin (33): A solution of **31** (5.0 mg, 0.0028 mmol) in $CHCl_3$ (10 cm^3) was admixed with a solution of $Ni(OAc)_2{\cdot}4H_2O$ (1.0 mg, 0.004 mmol) in MeOH (2.5 cm^3). The mixture was stirred with gentle reflux for 1 h. After being poured into water, the reaction mixture was extracted with $CHCl_3$, washed with brine, and then dried. The residue obtained after removal of solvent was chromatographed on silica gel (3.4×18 cm) with $CHCl_3$ afforded the Ni–Pd–Ni complex **37** (1.1 mg, 21%, see below) from the first fractions. Further fractions with $CHCl_3$–AcOEt (15 : 1) afforded the Ni–Pd–H_2 complex **33** (2.1 mg, 41%) and the starting material **31** (1.0 mg, 20%) successively.

33: Deep purple microcrystals (hexane–$CHCl_3$); Mp > 300 °C; Mass (FAB) *m/z* 1814 (M^++1); IR (KBr) 3310 (NH), 2960, 2930, and 2870 cm^{-1} (CH); ^1H NMR δ = 10.11 (2H, s, *meso*-H), 9.96 (2H, s, *meso*-H), 9.94 (1H, s, *meso*-H), 9.60 (1H, s, *meso*-H), 9.55 (2H, s, *meso*-H), 8.44 (1H, d, *J* = 15 Hz, –CH=CH–), 8.09 (1H, br d, *J* = 15 Hz, –CH=CH–), 8.01 (1H, d, *J* = 15 Hz, –CH=CH–), 7.79 (1H, br d, *J* = 15 Hz, –CH=CH–), 4.2—3.3 (48H, m, CH_2),

2.1—0.8 (72H, m, CH_3), and −2.89 (2H, br s, NH); Vis-uv λ_{max} 344 (sh 39000), 412 (300000), 424 (sh 275000), 509 (28200), 539 (32600), 572 (31300), 632 (4400), and WAB up to 800 nm. Found: C, 74.00; H, 7.68; N, 8.92%. Calcd for $C_{112}H_{134}N_{12}NiPd$: C, 74.18; H, 7.45; N, 9.27%.

Palladium(II)–Nickel(II)–FB Complex of (*E*,*E*)-5,15-Bis[2-(2,3,7,8,12,13,17,18-octaethyl-5-porphyrinyl)vinyl]-2,3,7,8,12,13,17,18-octaethylporphyrin (34): A solution of **29** (9.4 mg, 0.0055 mmol) in $CHCl_3$ (10 cm^3) was admixed with a solution of $Pd(OAc)_2$ (1.20 mg, 0. 0055 mmol) in MeOH (2.5 cm^3). The mixture was refluxed for 15 min. After being poured into water, the reaction mixture was extracted with $CHCl_3$, washed with brine, and then dried. The residue obtained after removal of solvent was chromatographed on silica gel (3.4×18 cm) with $CHCl_3$–AcOEt (20 : 1) to afford a trace of the Pd–Ni–Pd complex **40** (see below) as the first eluent. The fractions with $CHCl_3$ afforded the Pd–Ni–H_2 complex **34** (3.0 mg, 30%). The starting material **29** (4.0 mg, 43%) was recovered from the final fractions.

34: Black purple microcrystals (hexane–$CHCl_3$); Mp > 300 °C; Mass (FAB) *m/z* 1814 (M^++1); IR (KBr) 3300 (NH), 2960, 2930, and 2870 cm^{-1} (CH); ^{1}H NMR δ = 10.05 (4H, br s, *meso*-H), 10.02 (1H, s, *meso*-H), 9.91 (1H, s, *meso*-H), 9.45 (1H, s, *meso*-H), 9.44 (1H, s, *meso*-H), 8.13 (1H, d, *J* = 15 Hz, –CH=CH–), 8.05 (1H, d, *J* = 15 Hz, –CH=CH–), 8.04 (1H, d, *J* = 15 Hz, –CH=CH–), 7.84 (1H, d, *J* = 15 Hz, –CH=CH–), 4.2—3.4 (48H, m, CH_2), 2.0—0.5 (48H, m, CH_3), 1.3—1.1 (24H, m, CH_3), and −2.81 (1H, br s, NH); Vis-uv λ_{max} 277 (sh 30000), 300 (sh 29200), 334 (sh 41700), 411 (293000), 428 (sh 228000), 512 (48200), 553 (46500), 561 (sh 39200), 587 (sh 22300), 633 (sh 8400), and WAB up to 1000 nm. Found: C, 73.88; H, 7.71; N, 9.00%. Calcd for $C_{112}H_{134}N_{12}NiPd$: C, 74.18; H, 7.45; N, 9.27%.

Nickel(II)–Nickel(II)–Palladium(II) Complex of (*E*,*E*)-5,15-Bis[2-(2,3,7,8,12,13,17,18-octaethyl-5-porphyrinyl)vinyl]-2,3,7,8,12,13,17,18-octaethylporphyrin (35): A solution of **30** (4.0 mg, 0.0023 mmol) in $CHCl_3$ (10 cm^3) was admixed with a solution of $Pd(OAc)_2$ (3.6 mg, 0.016 mmol) in MeOH (2 cm^3). The mixture was stirred with gentle reflux for 30 min. After being poured into water, the reaction mixture was extracted with $CHCl_3$, washed with brine, and then dried. The residue obtained after removal of solvent was chromatographed on silica gel (3.4×8 cm) with $CHCl_3$ to afford the Ni–Ni–Pd complex **35** (3.4 mg, 80%) as the first eluent.

35: Deep purple microcrystals (hexane–$CHCl_3$); Mp > 300 °C; Mass (FAB) *m/z* 1871 (M^++1); IR (KBr) 2960, 2930, and 2870 cm^{-1} (CH); ^{1}H NMR δ = 10.02 (3H, very br s, *meso*-H), 9.48 (1H, very br s, *meso*-H), 9.45 (2H, very br s, *meso*-H), 9.39 (2H, very br s, *meso*-H), 7.99 (1H, very br s, –CH=CH–), 7.79 (1H, very br s, –CH=CH–), 7.61 (2H, very br s, –CH=CH–), 4.2—3.1 (48H, m, CH_2), and 2.0—0.8 (72H, m, CH_3). The signals due to all the meso and vinylene protons were still broad even at 50 °C; Vis-uv λ_{max} 336 (sh 42800), 408 (318000), 424 (sh 253600), 519 (50500), 554 (53000), 560 (sh 51000), 578 (sh 29000), and WAB up to 850 nm. Found: C, 71.68; H, 7.35; N, 8.72%. Calcd for $C_{112}H_{132}N_{12}Ni_2Pd$: C, 71.93; H, 7.11; N, 8.99%.

Nickel(II)–Nickel(II)–Platinum(II) Complex of (*E*,*E*)-5,15-Bis[2-(2,3,7,8,12,13,17,18-octaethyl-5-porphyrinyl)vinyl]-2,3,7,8,12,13,17,18-octaethylporphyrin (36): The mixture of **30** (7.5 mg, 0.0042 mmol) and $PtCl_2$ (8.9 mg, 0.033 mmol) in AcOH (8 cm^3) was refluxed for 4 h. After being poured into water and neutralized with sat. $NaHCO_3$ aq, the reaction mixture was extracted with $CHCl_3$, washed with brine, and then dried. The residue obtained after removal of solvent was chromatographed on silica gel (3.2×10 cm) with $CHCl_3$ to afford the Ni–Ni–Pt complex **36** (2.2 mg, 26%) from the first fractions. From the further fractions with $CHCl_3$–AcOEt (19 : 1) was recovered the starting material **30** (2.5 mg, 33%) along with some hardly soluble materials.

36: Deep purple microcrystals (hexane–$CHCl_3$); Mp > 300 °C; Mass (FAB) *m/z* 1959 (M^++1); IR (KBr) 2960, 2930, and 2860 cm^{-1} (CH); ^{1}H NMR δ = 9.95 (3H, very br s, *meso*-H), 9.45 (5H, very br d, *meso*-H), 7.94 (2H, very br d, *J* = 15 Hz, –CH=CH–), 7.62 (2H, very br d, *J* = 15 Hz, –CH=CH–), 4.1—3.2 (48H, m, CH_2), 2.1—1.9 (48H, m, CH_3), and 1.3—1.1 (24H, m, CH_3). The signals due to all the meso and vinylene protons were still very broad even at 50 °C; Vis-uv λ_{max} 300 (45000), 402 (279000), 424 (245000), 510 (59300), 543 (65500), 550 (sh 60200), 574 (sh 25400), and WAB up to 850 nm. Found: C, 68.73; H, 7.01; N, 8.55%. Calcd for $C_{112}H_{132}N_{12}Ni_2Pt$: C, 68.68; H, 6.79; N, 8.58%.

Nickel(II)–Palladium(II)–Nickel(II) Complex of (*E*,*E*)-5,15-Bis[2-(2,3,7,8,12,13,17,18-octaethyl-5-porphyrinyl)vinyl]-2,3,7,8,12,13,17,18-octaethylporphyrin (37): A solution of **31** (5.0 mg, 0.0028 mmol) in $CHCl_3$ (10 cm^3) was admixed with a solution of $Ni(OAc)_2 \cdot 4H_2O$ (10 mg, 0.04 mmol) in MeOH (2.5 cm^3). The mixture was stirred with gentle reflux for 1 h. After being poured into water, the reaction mixture was extracted with $CHCl_3$, washed with brine, and then dried. The residue obtained after removal of solvent was chromatographed on silica gel (3.4×8 cm) with $CHCl_3$ to afford the Ni–Pd–Ni complex **37** (3.2 mg, 60%) from the first fractions.

37: Bright purple microcrystals (hexane–$CHCl_3$); Mp > 300 °C; Mass (FAB) *m/z* 1871 (M^++1); IR (KBr) 2960, 2930, and 2870 cm^{-1} (CH); ^{1}H NMR δ = 9.84 (2H, s, *meso*-H), 9.51 (2H, s, *meso*-H), 9.46 (4H, s, *meso*-H), 7.89 (2H, d, *J* = 15 Hz, –CH=CH–), 7.69 (2H, br d, *J* = 15 Hz, –CH=CH–), 4.2—3.2 (48H, m, CH_2), and 2.0—0.6 (72H, m, CH_3); Vis-uv λ_{max} 344 (23000), 409 (296000), 425 (255000), 536 (25000), 569 (28000), and WAB up to 750 nm. Found: C, 71.73; H, 7.23; N, 9.05%. Calcd for $C_{112}H_{132}N_{12}Ni_2Pd$: C, 71.93; H, 7.11; N, 8.99%.

Nickel(II)–Palladium(II)–Palladium(II) Complex of (*E*,*E*)-5,15-Bis[2-(2,3,7,8,12,13,17,18-octaethyl-5-porphyrinyl)vinyl]-2,3,7,8,12,13,17,18-octaethylporphyrin (38): A solution of **32** (4.0 mg, 0.0021 mmol) in $CHCl_3$ (10 cm^3) was admixed with a solution of $Ni(OAc)_2 \cdot 4H_2O$ (3.7 mg, 0.015 mmol) in MeOH (2.5 cm^3). The mixture was stirred with gentle reflux for 1 h. After being poured into water, the reaction mixture was extracted with $CHCl_3$, washed with brine, and then dried. The residue obtained after removal of solvent was chromatographed on silica gel (3.4×8 cm) with $CHCl_3$ to afford the Ni–Pd–Pd complex **38** (3.1 mg, 75%) from the first fractions.

38: Reddish purple microcrystals (hexane–$CHCl_3$); Mp > 300 °C; Mass (FAB) *m/z* 1918 (M^++1); IR (KBr) 2960, 2930, and 2870 cm^{-1} (CH); ^{1}H NMR δ = 10.07 (2H, br s, *meso*-H), 10.04 (1H, s, *meso*-H), 9.96 (1H, s, *meso*-H), 9.94 (1H, s, *meso*-H), 9.59 (1H, s, *meso*-H), 9.54 (2H, s, *meso*-H), 8.13 (1H, d, *J* = 15 Hz, –CH=CH–), 8.02 (1H, br d, *J* = 15 Hz, –CH=CH–), 8.00 (1H, d, *J* = 15 Hz, –CH=CH–), 7.78 (1H, br d, *J* = 15 Hz, –CH=CH–), 4.4—3.3 (48H, m, CH_2), and 2.1—0.7 (72H, m, CH_3); Vis-uv λ_{max} 340 (41000), 409 (354000), 426 (316000), 534 (43000), 554 (sh 46000), and 563 nm (50000). Found: C, 69.89; H, 6.89; N, 8.57%. Calcd for $C_{112}H_{132}N_{12}NiPd_2$: C, 70.14; H, 6.94; N, 8.76%.

Nickel(II)–Palladium(II)–Platinum(II) Complex of (*E*,*E*)-5,15-Bis[2-(2,3,7,8,12,13,17,18-octaethyl-5-porphyrinyl)vinyl]-2,3,7,8,12,13,17,18-octaethylporphyrin (39): A solution of **33** (9.0 mg, 0.0050 mmol) in PhOH (5 cm^3) was heated at 150 °C for 30 min. Into this solution, [Pt(acac)$_2$] (15 mg, 0.038 mmol) was added at a time. The mixture was stirred at 150 °C for 5 h. After

being poured into water, the reaction mixture was extracted with $CHCl_3$. The extracts were washed with 1M NaOH aq (1 M = 1 mol dm^{-3}) followed by brine and then dried. The residue obtained after removal of solvent was chromatographed on silica gel (3.4×12 cm) with $CHCl_3$ to afford the Ni–Pd–Pt complex **39**[9] (3.1 mg, 32%), together with some hardly soluble materials.

39: Reddish purple microcrystals (hexane–$CHCl_3$); Mp > 300 °C; Mass (FAB) *m/z* 2007 (M^++1); IR (KBr) 2960, 2920, and 2850 cm^{-1} (CH); ^{1}H NMR δ = 9.99 (2H, br s, *meso*-H), 9.96 (2H, s, *meso*-H), 9.95 (1H, s, *meso*-H), 9.60 (1H, s, *meso*-H), 9.55 (2H, br s, *meso*-H), 8.19 (2H, d, J = 15 Hz, –CH=CH–), 8.01 (2H, d, J = 15 Hz, –CH=CH–), 7.97 (2H, br d, J = 15 Hz, –CH=CH–), 7.78 (2H, d, J = 15 Hz, –CH=CH–), 4.3—3.2 (48H, m, CH_2), and 2.2—0.7 (72H, m, CH_3); Vis-uv λ_{max} 347 (42500), 393 (sh 296000), 404 (331500), 426 (318000), 513 (sh 33800), 533 (sh 48700), 543 (65000), 552 (sh 54000), 568 (38800), and WAB up to 700 nm. Found: C, 67.22; H, 6.96; N, 8.44%. Calcd for $C_{112}H_{132}N_{12}NiPdPt$: C, 67.04; H, 6.63; N, 8.38%.

Palladium(II)–Nickel(II)–Palladium(II) Complex of (*E,E*)-5, 15-Bis[2-(2,3,7,8,12,13,17,18-octaethyl-5-porphyrinyl)vinyl]-2, 3,7,8,12,13,17,18-octaethylporphyrin (40): A solution of **29** (6.0 mg, 0.0035 mmol) in $CHCl_3$ (10 cm^3) was admixed with a solution of $Pd(OAc)_2$ (11.4 mg, 0.051 mmol) in MeOH (2.5 cm^3). The mixture was stirred with gentle reflux for 30 min. After being poured into water, the reaction mixture was extracted with $CHCl_3$, washed with brine, and then dried. The residue obtained after removal of solvent was chromatographed on silica gel (3.4×8 cm) with $CHCl_3$ to afford the Pd–Ni–Pd complex **40** (4.7 mg, 70%) as the first eluent.

40: Black purple microcrystals (hexane–$CHCl_3$); Mp > 300 °C; Mass (FAB) *m/z* 1918 (M^++1); IR (KBr) 2960, 2930, and 2870 cm^{-1} (CH); ^{1}H NMR δ = 10.04 (4H, br s, *meso*-H), 10.02 (2H, s, *meso*-H), 9.47 (2H, s, *meso*-H), 8.01 (2H, d, J = 15 Hz, –CH=CH–), 7.85 (2H, br d, J = 15 Hz, –CH=CH–), 4.2—3.1 (48H, m, CH_2), and 2.1—0.8 (72H, m, CH_3); Vis-uv λ_{max} 354 (35500), 408 (311000), 424 (253000), 523 (39800), 553 (57700), 562 (sh 51600), 588 (sh 19900), and WAB up to 800 nm. Found: C, 69.89; H, 7.11; N, 8.65%. Calcd for $C_{112}H_{132}N_{12}NiPd_2$: C, 70.14; H, 6.94; N, 8.76%.

Palladium(II)–Nickel(II)–Platinum(II) Complex of (*E,E*)-5, 15-Bis[2-(2,3,7,8,12,13,17,18-octaethyl-5-porphyrinyl)vinyl]-2, 3,7,8,12,13,17,18-octaethylporphyrin (41): A solution of **34** (6.8 mg, 0.0038 mmol) and $PtCl_2$ (6.8 mg, 0.026 mmol) in AcOH (10 cm^3) was refluxed for 10 h. After being poured into water, the reaction mixture was extracted with $CHCl_3$, washed with brine, and then dried. The residue obtained after removal of solvent was chromatographed on silica gel (3.4×8 cm) with $CHCl_3$ to afford the Pd–Ni–Pt **41** (2.2 mg, 29%) from the first fractions and then with $CHCl_3$–AcOEt (97 : 3) to afford the starting material **34** (3.1 mg, 46%) from the second fractions.

41: Sparkling reddish purple microcrystals (hexane–$CHCl_3$); Mp > 300 °C; Mass (FAB) *m/z* 2007 (M^++1); IR (KBr) 2960, 2930, and 2870 cm^{-1} (CH); ^{1}H NMR δ = 10.03 (2H, s, *meso*-H), 10.02 (2H, s, *meso*-H), 9.96 (2H, br s, *meso*-H), 9.48 (2H, s, *meso*-H), 8.01 (2H, d, J = 15 Hz, –CH=CH–), 7.97 (2H, d, J = 15 Hz, –CH=CH–), 7.90 (2H, d, J = 15 Hz, –CH=CH–), 7.85 (2H, d, J = 15 Hz, –CH=CH–), 4.1—3.0 (48H, m, CH_2), and 2.1—0.8 (72H, m, CH_3); Vis-uv λ_{max} 336 (42400), 401 (330000), 425 (298000), 517 (47300), 543 (sh 66000), 551 (73000), 562 (sh 47000), 587 (sh 20400), and WAB up to 700 nm. Found: C, 66.88; H, 6.78; N, 8.15%. Calcd for $C_{112}H_{132}N_{12}NiPdPt$: C, 67.04; H, 6.63; N, 8.38%.

Financial support by a Grant-in-Aid for Scientific Research No. 11640528 from the Ministry of Education, Science, Sports and Culture, is gratefully acknowledged.

References

1 M. R. Wasielewski, *Chem. Rev.*, **92**, 435 (1992); J. L. Sessler, V. L. Capuano, and A. Harriman, *J. Am. Chem. Soc.*, **115**, 4618 (1993); A. Osuka, N. Tanabe, S. Kawabata, I. Yamazaki, and Y. Nishimura, *J. Org. Chem.*, **60**, 7177 (1995); P. J. Angiolillo, V. S. -V. Lin, J. M. Vanderkooi, and M. J. Therien, *J. Am. Chem. Soc.*, **117**, 12514 (1995); A. Giraudeau, L. Ruhlmann, L. E. Kahef, and M. Gross, *J. Am. Chem. Soc.*, **118**, 2969 (1996); J. P. Strachan, S. Gentemann, J. Seth, W. A. Kalsbeck, J. S. Lindsey, D. Holten, and D. F. Bocian, *J. Am. Chem. Soc.*, **119**, 11191 (1997); O. Mongin, C. Papamicael, N. Hoyler, and A. Gossauer, *J. Org. Chem.*, **63**, 5568 (1998); R. W. Wagner, J. Seth, S. I. Yang, D. Kim, D. F. Bocian, D. Holton, and J. S. Linsey, *J. Org. Chem.*, **63**, 5042 (1998); H. Levanon, T. Galili, A. Regev, G. P. Wiederrecht, W. A. Svec, and M. R. Wasielewski, *J. Am. Chem. Soc.*, **120**, 6366 (1998); H. Imahori, H. Yamada, S. Ozawa, K. Ushida, and Y. Sakata, *Chem. Commun.*, **1999**, 1165; M. Fujitsuka, O. Ito, H. Imahori, K. Yamada, H. Yamada, and Y. Sakata, *Chem. Lett.*, **1999**, 721, and many other references cited therein.

2 H. Higuchi, K. Shimizu, J. Ojima, K. Sugiura, and Y. Sakata, *Tetrahedron Lett.*, **36**, 5359 (1995).

3 G. V. Ponomarev and A. M. Shul'ga, *Khim. Geterotski. Soed.*, **1986**, 278; G. V. Ponomarev, D. V. Yashunsky, and D. P. Arnold, *Recent Res. Devl. Pure Appl. Chem.*, **2**, 199 (1998).

4 H. Higuchi, K. Shimizu, M. Takeuchi, J. Ojima, K. Sugiura, and Y. Sakata, *Bull. Chem. Soc. Jpn.*, **70**, 1923 (1997).

5 J. W. Buchler, in "The Porphyrins," ed by D. Dolphin, Academic Press, New York (1978), Vol. I, pp. 389—483.

6 H. Higuchi, M. Shinbo, M. Usuki, M. Takeuchi, Y. Hasegawa, K. Tani, and J. Ojima, *Bull. Chem. Soc. Jpn.*, **72**, 1887 (1999).

7 a) For nickelation: J. W. Buchler and L. Puppe, *Liebigs Ann. Chem.*, **1970**, 142. b) For palladation and platination: J. W. Buchler and L. Puppe, *Liebigs Ann. Chem.*, **1974**, 1046.

8 G. V. Ponomarev, V. V. Borovkov, K. Sugiura, Y. Sakata, and A. M. Shul'ga, *Tetrahedron Lett.*, **34**, 2153 (1993).

9 H. Higuchi, M. Takeuchi, Y. Hasegawa, and J. Ojima, *Nonlinear Optics*, **22**, 333 (1999).

10 H. Fischer and W. Neumann, *Justus Liebigs Ann. Chim.*, **494**, 225 (1932); J. W. Buchler and L. Puppe, *Justus Liebigs Ann. Chim.*, **494**, 225 (1932); T. R. Johnson and J. J. Kats, in "The Porphyrins," ed by D. Dolphin, Academic Press, New York (1978), Vol. IV, pp. 1—59.

11 H. Higuchi, M. Takeuchi, and J. Ojima, *Chem. Lett.*, **1996**, 593.

12 K. Maruyama, T. Nagata, and A. Osuka, *J. Phys. Org. Chem.*, **1988**, 63.

13 R. Takigawa, Y. Kai, G. V. Ponomarev, K. Sugiura, V. V. Borovkov, T. Kaneda, and Y. Sakata, *Chem. Lett.*, **1993**, 1071.

14 Jurgen-H. Fuhrhop, K. M. Kadish, and D. G. Davis, *J. Am. Chem. Soc.*, **95**, 5140 (1973).

15 D. P. Arnold, V. V. Borovkov, and G. V. Ponomarev, *Chem. Lett.*, **1996**, 485.

16 K. Sugiura, G. V. Ponomarev, S. Okubo, A. Tajiri, and Y. Sakata, *Bull. Chem. Soc. Jpn.*, **70**, 1115 (1997).